ARL-TR-9845 ● Dec 2023

Parametric Study of Design Characteristics for Neutron Interrogation of Materials by Analysis of Gamma Spectra

by Nusrat Sarwahrdy, Ryan Brockington, Jason Barbier, and Marc Litz

NOTICES

Disclaimers

The findings in this report are not to be construed as an official Department of the Army position unless so designated by other authorized documents.

Citation of manufacturer's or trade names does not constitute an official endorsement or approval of the use thereof.

Destroy this report when it is no longer needed. Do not return it to the originator.

ARL-TR-9845 ● DEC 2023

Parametric Study of Design Characteristics for Neutron Interrogation of Materials by Analysis of Gamma Spectrum

Nusrat Sarwahrdy and Jason Barbier
University of Maryland

Ryan Brockington
United States Military Academy

Marc Litz
DEVCOM Army Research Laboratory

REPORT DOCUMENTATION PAGE

1. REPORT DATE	2. REPORT TYPE	3. DATES COVERED	
		START DATE	END DATE
December 2023	Technical Report	May 26, 2022	August 3, 2022

4. TITLE AND SUBTITLE
Parametric Study of Design Characteristics for Neutron Interrogation of Materials by Analysis of Gamma Spectrum

5a. CONTRACT NUMBER	5b. GRANT NUMBER	5c. PROGRAM ELEMENT NUMBER
5d. PROJECT NUMBER	5e. TASK NUMBER	5f. WORK UNIT NUMBER

6. AUTHOR(S)
Nusrat Sarwahrdy, Ryan Brockington, Jason Barbier, and Marc Litz

7. PERFORMING ORGANIZATION NAME(S) AND ADDRESS(ES)	8. PERFORMING ORGANIZATION REPORT NUMBER
DEVCOM Army Research Laboratory ATTN FCDD-RLA-GC Adelphi, MD 20783-1138	ARL-TR-9845

9. SPONSORING/MONITORING AGENCY NAME(S) AND ADDRESS(ES)	10. SPONSOR/MONITOR'S ACRONYM(S)	11. SPONSOR/MONITOR'S REPORT NUMBER(S)

12. DISTRIBUTION/AVAILABILITY STATEMENT
DISTRIBUTION STATEMENT A. Approved for public release: distribution unlimited.

13. SUPPLEMENTARY NOTES
ORCID ID: Marc Litz, 0000-0003-0694-4152

14. ABSTRACT
The technique of neutron interrogation of materials enables a description of the elemental composition of soil and its components. Neutrons from an electronic neutron generator interact with atomic nuclei causing the production of characteristic gamma rays that identify the composition of a material volume. Determination of the elemental composition has wide-ranging applications in environmental science, planetary science, and lunar science. Detection of nitrogen-based explosives is crucial to Soldier safety. NASA has determined the chemical composition of lunar and planetary soil for use in understanding the development of the solar system. Simulation geometries and material composition within Monte Carlo N-Particle Transport are varied. The simulation geometry (source, shield, target, and detector) is optimized to maximize photon flux in the detector as well as maximize neutron flux in target. The depth of the target in soil is varied and quantified. The neutron flux in the target volume varies 93% over a 2-ft depth. A parametric study of detector height above the soil found that 10 cm maximizes photon flux. A 28-cm shielding radius resulted in 90% reduction of neutron flux in cerium(III) bromide ($CeBr_3$). Prominent energies in gamma spectrum in $CeBr_3$ detector are identified.

15. SUBJECT TERMS
Energy Sciences, nuclear sciences, neutron interrogation, standoff detection, soil composition, neutron shielding

16. SECURITY CLASSIFICATION OF:			17. LIMITATION OF ABSTRACT	18. NUMBER OF PAGES
a. REPORT	b. ABSTRACT	C. THIS PAGE		
UNCLASSIFIED	UNCLASSIFIED	UNCLASSIFIED	UU	75

19a. NAME OF RESPONSIBLE PERSON	19b. PHONE NUMBER *(Include area code)*
Marc Litz	(301) 980-0405

STANDARD FORM 298 (REV. 5/2020)
Prescribed by ANSI Std. Z39.18

Contents

List of Figures

List of Tables

1. Introduction

Neutron interrogation techniques are used to determine the elemental composition of a material. A deuterium–deuterium (DD)-type electronic neutron generator accelerates deuterium plasma into a deuterium-impregnated solid target generating 2.45-MeV neutrons.[1] When neutrons collide with an atom, four different reactions can occur. One reaction is inelastic scattering $(n, n'\gamma)$. Inelastic scattering occurs when neutrons collide with the nucleus of an atom, and the incoming neutrons are absorbed into the nucleus exciting it. When the compound nucleus de-excites, it emits a neutron of lower energy as well as one or more gamma photons. The compound nucleus can also de-energize by emitting either a proton or an alpha particle. This reaction is called the transmutation reaction, $(n, p\gamma)$ or $(n, \alpha\gamma)$. Radiative capture (n, γ) occurs when the compound nucleus emits only gamma photons. Elastic scattering (n, n) (Fig. 1) occurs when the neutron colliding transfers some of its energy to the nucleus and reflects off in a different direction.[2]

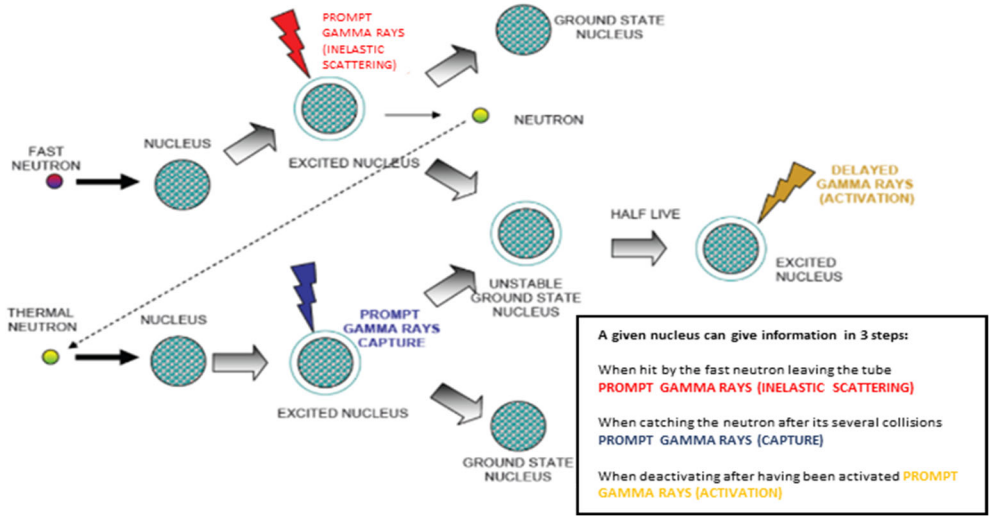

Fig. 1 Fast neutrons are compared to slow neutrons in the way they interact with a nucleus. Neutrons are captured after they have been slowed by scattering.[1]

The Army uses neutron interrogation to find explosives buried in soil. Neutron interrogation is a valuable technique that can be utilized in several other applications. For example, the Department of Agriculture is utilizing neutron interrogation technics to understand carbon profile in soil to improve the quality of soil for agricultural purposes. Neutron interrogation is most prominently used in space exploration because soil composition can tell the history of extraterrestrial planets. NASA's Lunar Prospector mission used a gamma ray spectrometer (GRS) and neutron spectrometer (NS). The GRS data were used to determine elemental composition of lunar surface, specifically major oxides. The NS data were used to

determine lunar surface parameters such as soil density, composition, and mass of lunar surface materials. Using the GRS and NS data, scientists found oxides such as MgO, TiO_2, FeO, and elements K and Th. The moon has less abundance of volatiles relative to terrestrial planets. Scientists also found a very high abundance of MgO and low abundance of TiO_2.[3] After the Lunar Prospector mission, NASA launched the Lunar Reconnaissance Orbiter (LRO) mission with a Lunar Exploration Neutron Detector (LEND) onboard. The LEND data were used to collimate signals of epithermal neutrons in lunar soil. LEND found that variation of epithermal neutron flux (nFlux) across the lunar surface is very small. They also found that Fe-rich soil, in lunar surface, is producing faster neutrons compared with Al-rich soils.[4]

To shield the detector from neutron damage, 33% boron (B) doped, 0.918 g/cc, high-density polyethylene (HDPE) shield is used in simulations discussed in this paper. High-density polyethylene is inexpensive, and the hydrogen and boron in HDPE have high neutron-capture cross sections. Hydrogen (H) captures neutron through the $^1\mathrm{H}(n,\gamma)$ reaction and has a cross section of 0.33 barns for 0.027-eV neutrons in thermal equilibrium.[5] Boron is also a good absorber of neutrons because it has an even higher neutron absorption cross section of 3837 barns for 0.025-eV neutrons. When a ^{10}B nucleus captures a thermal neutron (0.25 eV) and undergoes fission,[6] two possible reactions are shown here:

$$^{10}B + n_{th}(0.025\ eV) \rightarrow\ \ ^4He +\ ^7Li + 2.79\ MeV\ (6\%)$$

$$^{10}B + n_{th}(0.025\ eV) \rightarrow\ \ ^4He +\ ^7Li + 2.31\ MeV +\ \gamma\ (0.478\ MeV)\ (94\%)$$

For both reactions, the α particle is absorbed by the shield, whereas the gamma rays pass through the shield.

In this report, we describe a series of parametric studies that include shielding thickness and position of detectors (Table 1). One goal is to minimize nFlux in the $CeBr_3$ detector from the neutron source. The thickness of the HDPE radiation shield around the neutron source is varied. The neutron (minimize) and photon (maximize) flux in the detector is calculated as a function of the HDPE shield radius. Moreover, the depth of the target location in the soil is varied, and the nFlux in the target is calculated at each depth level.

The nFlux energy profile in the target is also calculated as a function of depth in the dirt. Thermal neutrons are preferred because their cross section is greater than energetic neutrons. The gamma spectra in the detector are calculated and correlated to these target depths.

Next, we maximize photon flux (pFlux) in the detector by variation of detector radius from the neutron source and height above the ground (Sections 3.3 and 3.4).

The goal is to maximize pFlux in the detector and minimize nFlux in the detector. Minimizing nFlux reduces neutron degradation of the detector material, although $CeBr_3$ (Fig. 2) is one of the more radiation-tolerant materials. In Section 3.5, we vary the height of the neutron source above the ground with the goal of optimizing gamma signal from target into detector.

Table 1 Five-parameter variation involving source, shield, and detector geometry

Parameter	Histories (M)	Sources	Target	Detector	Comment
Shield radius	5	Neutron	. . .	nFlux, pFlux	• 28-cm HDPE radius reduces nFlux in detector by 90%. • nFlux decreases as soil depth increases.
Target depth	3	Neutron	nFlux	nFlux	• Thermal flux reduces linearly with depth as measured in the target. • Ratio of thermals to 2.5 MeV (DD) neutrons increases with depth. • DD flux reduces exponentially with depth as measured in the target.
Detector height	100	Gamma	. . .	pFlux	• pFlux maximizes 10 cm above soil.
Shield height	1.8	Gamma	. . .	pFlux	• pFlux maximizes shield 10 cm above soil.
Source height	68	Neutron	nFlux	nFlux, pFlux	• 11 cm maximizes nFlux in target. • 19-cm neutron source minimizes nFlux in CeBr. • pFlux remains relatively constant.

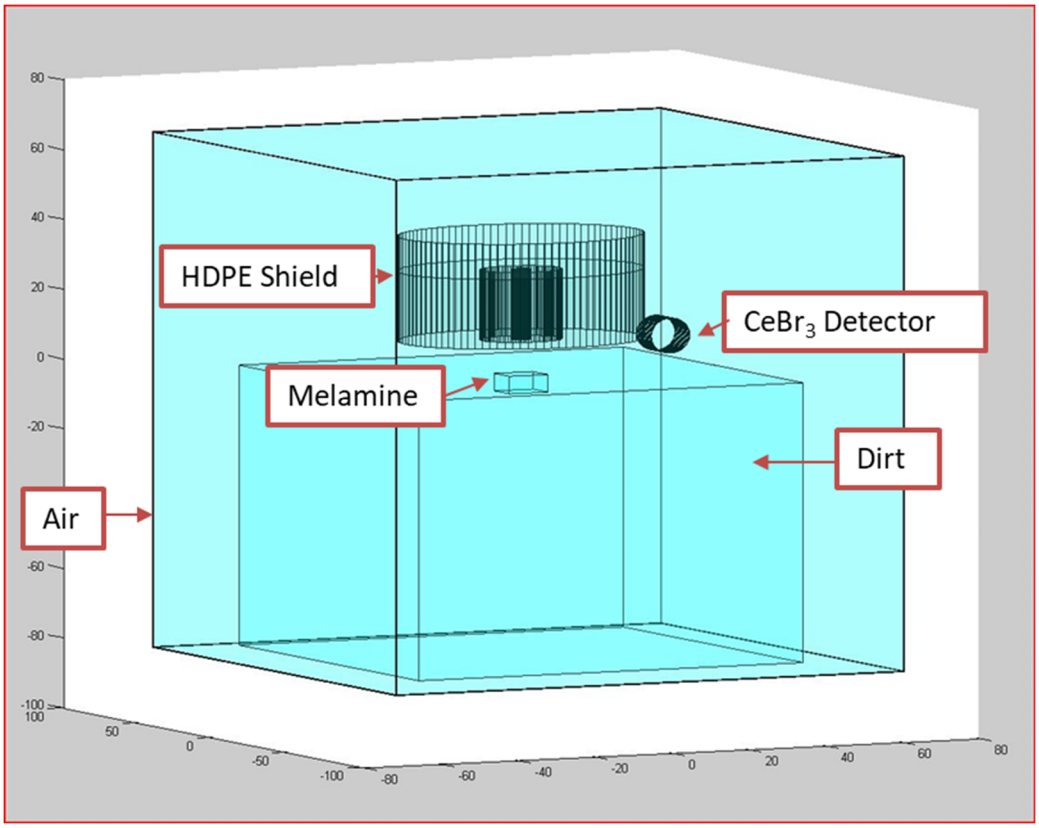

Fig. 2 Geometry of the simulation. The detector and the shield are 10 cm above soil. Target is in the first layer of soil. Neutron source is being varied inside the shield structure.

2. Approach

Monte Carlo N-Particle Transport (MCNP) version 6.2 is used for all simulation calculations. The MCNP is a legacy code developed by Los Alamos National Laboratory and uses the Monte Carlo method for radiation transport and scattering to track different particle types over various ranges of energy.

Monte Carlo simulations are randomly evolving simulations that use a random subset of possibility to simulate a situation. The law of large numbers states that simulations approach a true representation of reality as the number of runs are increased.[7] The MCNP tracks particles from a source location through the various particle interaction processes such as absorption and scattering. Each interaction in MCNP has a probability distribution function (PDF) associated with it. The MCNP picks a random number and compares the value to the PDF to determine which event occurs. Depending on how the random number compares to the PDF, it determines the next outcome of the process. The error associated with a Monte Carlo calculation is very sensitive to the number of trials performed.[8]

An MCNP output file creates a tally section consisting of energy bin, flux/energy deposited, and relative error of the mean. The tally creates energy bins with the desired resolution and outputs the mean flux/energy deposition of a bin.

Equation 1 shows the formula MCNP uses to calculate the standard deviation of the mean (from the tally), where N is the number of trials, x_i is the value of current run, and μ is the mean. The formula for mean calculation is shown in Eq. 2.

$$\sigma = \sqrt{\frac{1}{N}\sum_{i=1}^{N}(x_i - \mu)^2} \tag{1}$$

$$\mu = \frac{\sum_{i=1}^{N} x_i}{N} \tag{2}$$

Equation 3 shows that the variation in x_i is measured by the standard deviation of the histories that were run.

$$\sigma_\mu^2 = \frac{1}{N}\sigma^2 \tag{3}$$

By the central limit theorem,[7] if enough simulation histories are run the variation of the mean from each simulation history will be normally distributed about the expected mean.

Using the relative error of the mean from tally, R, the standard deviation can be calculated using Eq. 4. Since R is approximately $\frac{1}{\sqrt{N}}$, it is further emphasized that many histories are required to achieve statistical validity.[9]

$$\sigma^2 = R\sigma_\mu^2 \tag{4}$$

$$FOM = \frac{1}{R^2 T} \tag{5}$$

Along with relative error, MCNP also generates the statistical figure of merit (FOM). Equation 5 shows the formula for FOM, where R is the relative error of the mean and T is the simulation time.[9]

3. Results

3.1 Shield Radius

The isotropic neutron source in the simulation creates nFlux in the soil (neutrons that are scattering off soil can be detected by the $CeBr_3$ detector). Since the goal is to detect pFlux in $CeBr_3$, any form of neutron detection in the detector creates noise. In addition, due to nFlux exposure, the scintillator detector is damaged over time,

which leads to a decrease in the optical transmission of neutrons. For the first set of simulations, 90% was arbitrarily chosen as the base line of nFlux reduction in the $CeBr_3$ detector. One way of reducing nFlux is to use shielding in front of the $CeBr_3$ detector.

The melamine block is a 5- × 5-cm^2 block with a thickness of 5 cm. The soil consists of six layers. The neutron source is a 2.5-MeV isotropic disk source with a radius of 1 cm. This source is placed 20 cm above the ground. The neutron source is encapsulated with an HDPE shield (Fig. 3). To minimize nFlux in the detector, the HDPE shield radius was varied in the photon emission area. We chose a minimum size of 10-cm radius HDPE shield to easily accommodate the neutron generator. The HDPE shield radius varied from 10 to 35 cm in 5-cm increments (Fig. 4). Simulations were run with and without soil (just air) to account for neutron reflection from the soil as well.

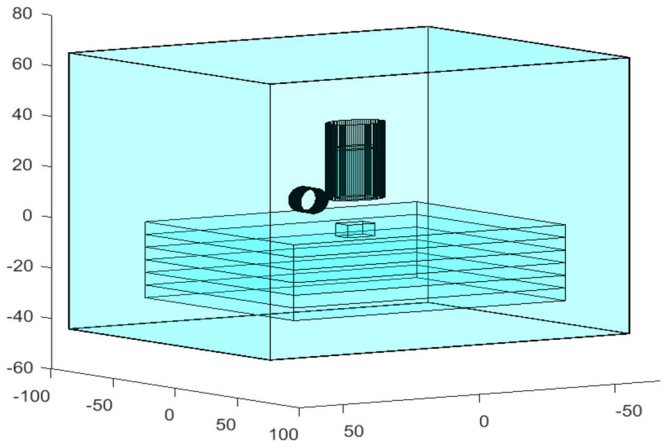

Fig. 3 Geometry of simulation is shown in centimeters. A melamine block is embedded in six layers of soil.

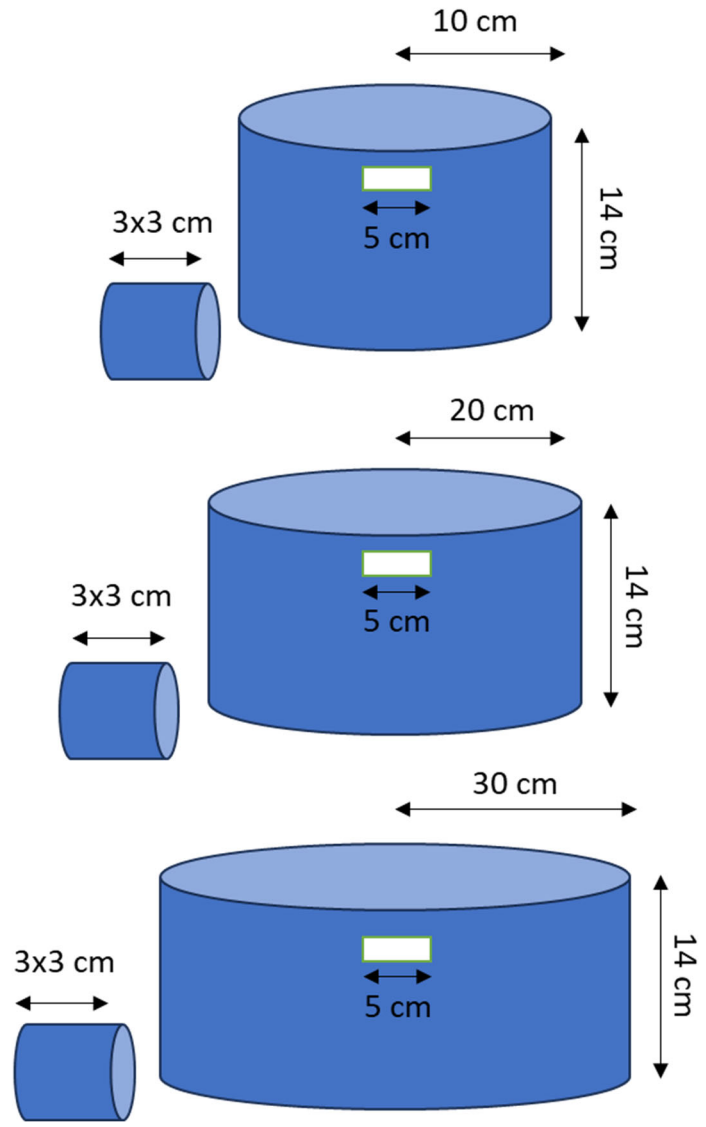

Fig. 4 Shield size variation and dimensions. Not drawn to scale.

Figure 5 shows the percentage of nFlux detected in the $CeBr_3$ detector as the shield radius is increased. This simulation was run without soil (just air) to observe trends in nFlux due to varying HDPE shield radius. Neutron flux in the detector decreased exponentially, and not as $1/r^2$, as shield radius was increased. We believe this difference is due to scattering of neutrons and photons occurring in the shielding and in the air, which departs from a perfect isotropic geometry. A similar trend is observed for pFlux and neutron energy deposition. A reduction in nFlux to 10% of the initial value is calculated when the radius of the shield was 30 cm. A 20% reduction in pFlux of initial was calculated when the HDPE shielding radius was 35 cm.

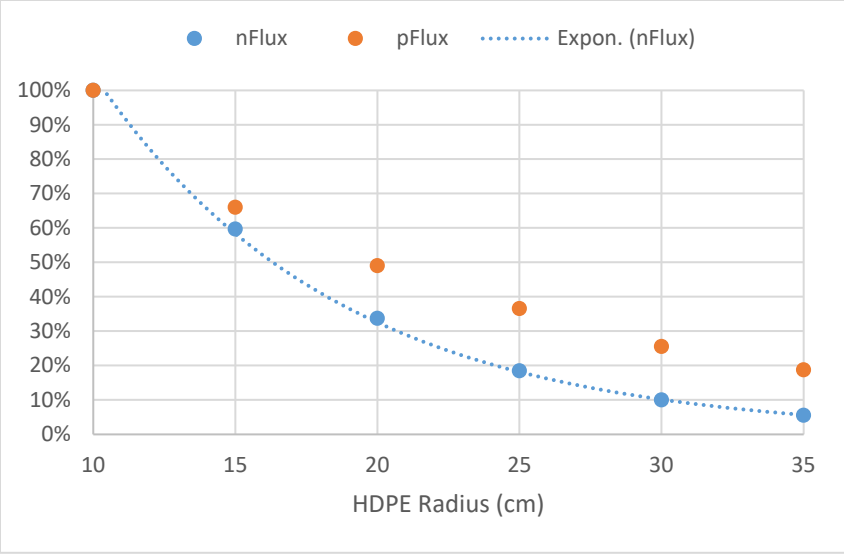

Fig. 5 The nFlux and pFlux are calculated on $CeBr_3$ where soil is replaced with air. The error bars are hidden by the plotting marker. nEdep = neutron energy deposition.

Simulation with soil was also run to account for neutron back scatter from the soil. Figure 6 shows comparison between nFlux versus shield radius with soil and without soil. Similarly, to the result found in Fig. 5, the 30-cm shield radius reduces nFlux in $CeBr_3$ by 90%. Figure 6 also shows that at a 30-cm shield radius, $CeBr_3$ detects 38% more nFlux with soil, which implies that approximately 38% of neutrons in the $CeBr_3$ detector are reflected neutrons from the soil.

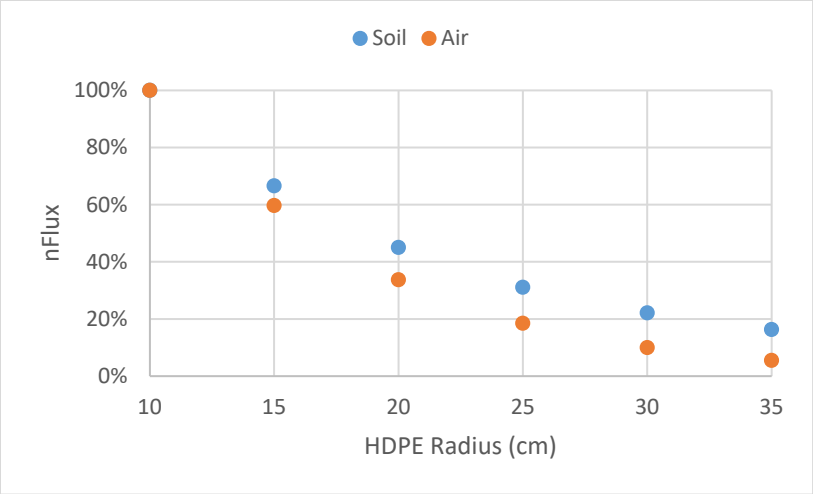

Fig. 6 Incremental increases in nFlux from soil vs. air. Error bars are hidden by plotting markers.

3.2 Target Depth

Deeper into soil, neutron energy changes (reduces) due to scattering. (Energy of gamma's are dependent upon the energy of neutrons.) Hence, it is valuable to quantify nFlux in soil to determine the percentage of low-energy neutrons to high-energy neutrons. This section will explore the relationship of change in nFlux with depth of target in soil.

The melamine target (Fig. 7) is a 5- × 5-cm block with a thickness of 5 cm. The neutron source is a 2.5-MeV isotropic disk source with a radius of 1 cm placed 20 cm above the ground. The neutron source is encapsulated with an HDPE radiation shield. The soil depth is increased to 32 inches to reduce any reflection of neutrons in soil. The target is varied through 12 layers of soil, and each layer is 2-inches (5-cm) thick (Fig. 8). See Appendix B for the MCNP input deck.

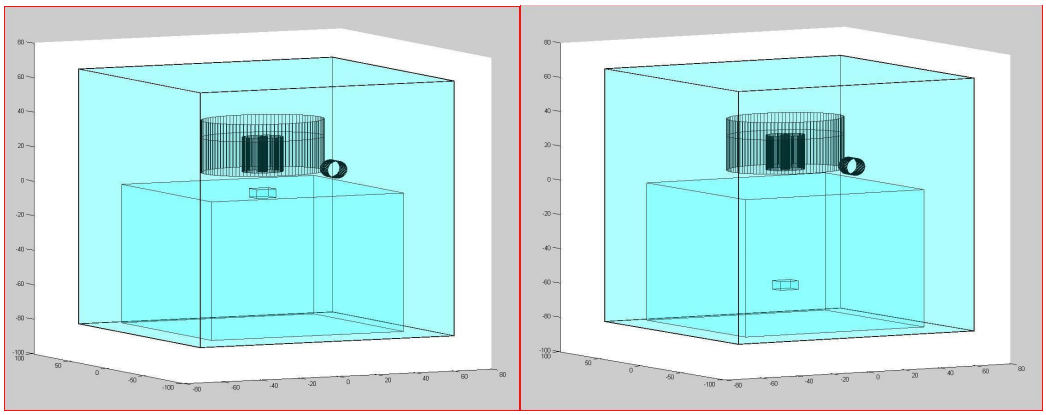

a) b)

Fig. 7 Simulation geometry. a) Initial position of melamine target. b) Final position of melamine target.

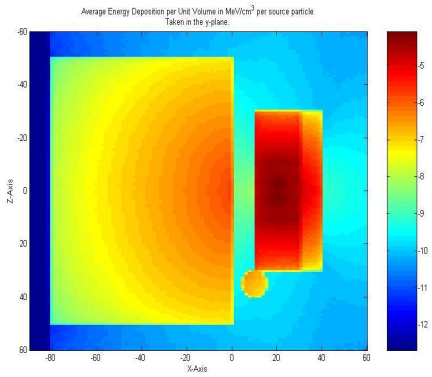

Fig. 8 Neutron flux gradient through six 2-inch layers of soil is shown. The mesh plot is captured in the xz axis. The units of energy deposition are MeV/g.

Neutron flux decays exponentially as the target is placed deeper into soil (Fig. 9). This indicates the effect that neutron scattering is amplified as the target is located deeper into soil. The spectrum neutron energy is shown in Fig. 10.

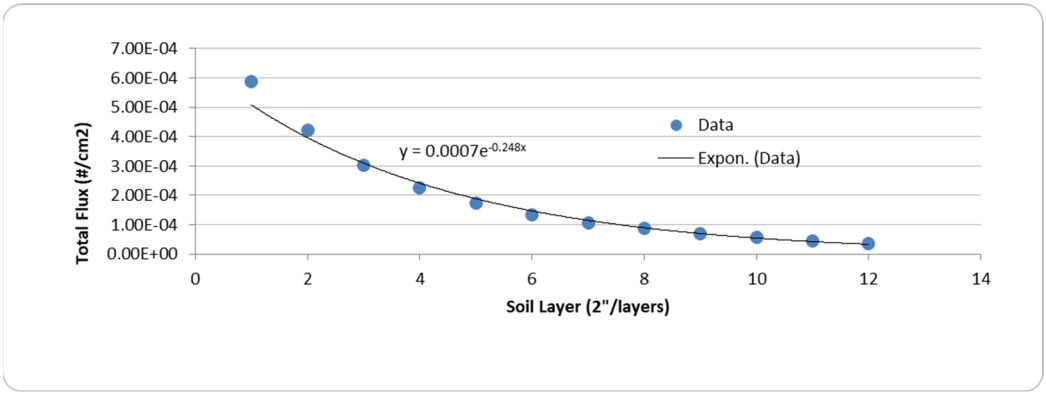

Fig. 9 Total nFlux vs. soil layer. The error bars are hidden by the plotting marker.

In successive layers of soil 2.5-MeV DD neutrons flux decreases (Fig. 10). In successive layers of soil 0.25-MeV neutrons flux increases. This implies that there are more low-energy neutrons deeper into soil than high-energy or 2.5-MeV DD neutrons. Low-energy neutrons are defined as those tracked below 1 keV, and high-energy neutrons are defined as those emitted at 2.5 MeV.

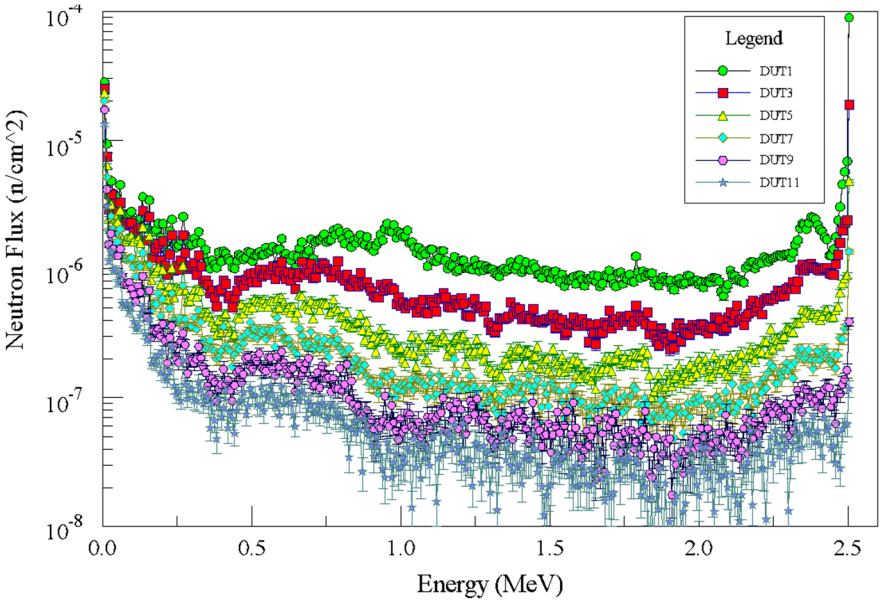

Fig. 10 Neutron flux at all energies at a melamine target as depth is increased. Soil layers 2, 4, 6, 8, 10, and 12 were omitted for clarity.

Figure 11 shows the spectrum of both low-energy and 2.5-MeV nFlux decreases in a melamine target as the target moves deeper into soil. When total nFlux of Fig. 11 is plotted, exponential decrease in 2.5-MeV neutrons and linear decrease in low-energy neutrons are calculated as the target is located deeper in the soil (Fig. 12). Overall, negative correlation is also seen as neutron energy increases between soil layer 12 and 1. Thus, both thermal and low-energy neutrons are at a higher concentration than DD neutrons at greater depths.

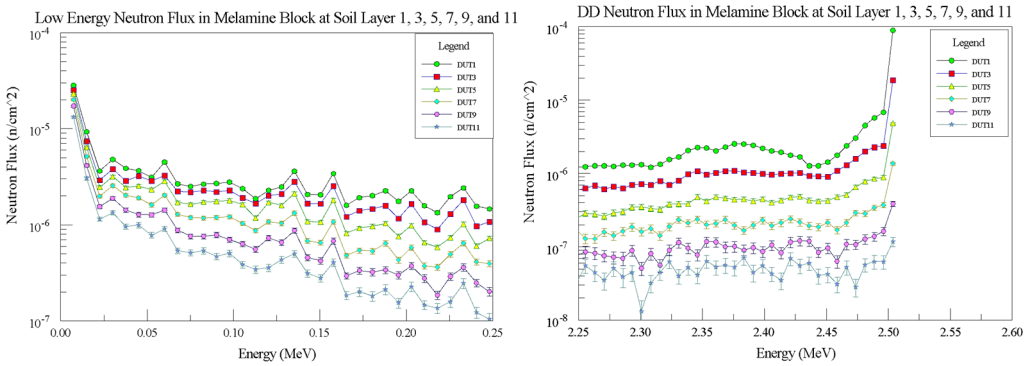

a) b)

Fig. 11 The low-energy and DD nFlux at the melamine target as depth is increased. The low-energy nFlux is displayed in graph a) while the high-energy, including DD, nFlux is displayed in graph b).

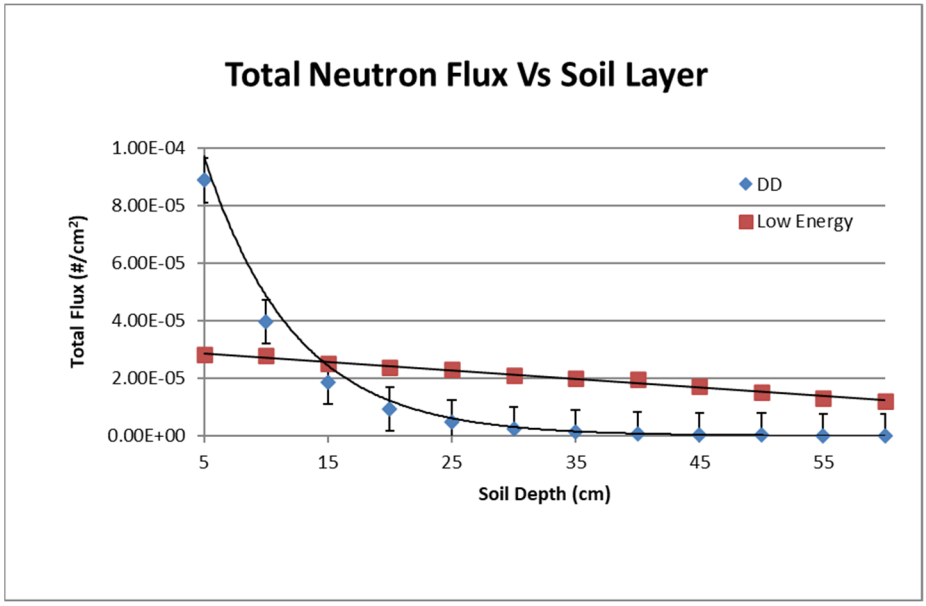

Fig. 12 The low-energy and DD nFlux at the melamine target as depth is increased. Both low-energy nFlux and DD nFlux are displayed.

The reaction in nFlux with depth is fit to the following curve (Eq. 6 fits DD neutron curve [Fig. 12]):

$$DD = A * b^{x} \tag{6}$$

Equation 7 fits low-energy (less than 1 keV) curve (Fig. 12).

$$Low\ Energy = m * x\ + b \tag{7}$$

To eliminate statistical discrepancy, longer history (27 Mh) simulation data, in soil layer 12, were compared to shorter history (3 Mh) simulation data. In Fig. 13, 3-Mh run shows a greater error and scatter of nFlux compared to 27-Mh run. The main reason for this difference was the number of histories run in the simulation. When the variance of nFlux of the same simulation runs was compared (Fig. 14), 3-Mh run shows higher and more volatile variances than 27-Mh run. Although 3-Mh run had more scatter data than 27 Mh, the overall trend of the two graphs is very similar. Hence, statistics did not hinder the initial assessment of the simulation results.

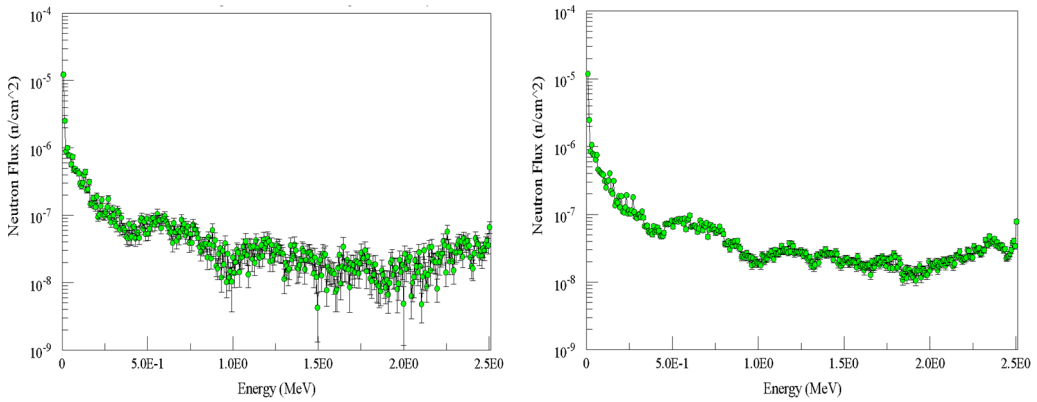

Fig. 13 Neutron flux is calculated in a melamine target at soil layer 12. An MCNP run was conducted at 3 Mh (~1 h), which is displayed in a). A comparison calculation executed for 27 Mh (~9 h) is displayed in b).

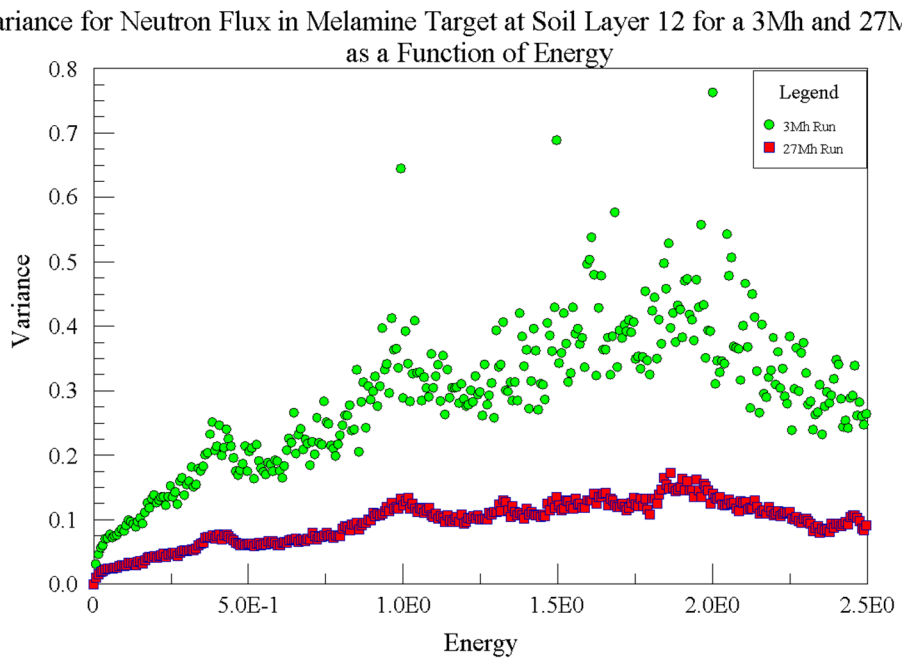

Fig. 14 The respective variances of the 3- and 27-Mh layer 12 runs from Fig. 12

3.3 $CeBr_3$ Position Along HDPE Shield

In Sections 3.3 and 3.4, gammas were sourced from target instead of neutrons inside shield (Appendix C for MCNP input deck). Gamma sources are used to reduce the run time and calculate the detector efficiency across this selected (although representative) gamma spectrum.

Varying Detector Height

Six gamma energies were chosen (470, 2223, 3540, 4432, 7100, and 10,800 keV) and sourced at location of the melamine target. These energies represent the boron, hydrogen, silicon, carbon, and iron gamma lines generated from material. This simulation is designed to vary the $CeBr_3$ detector (Fig. 15) height to find the optimal height of the detector where it can detect the most photons emitted from the target.

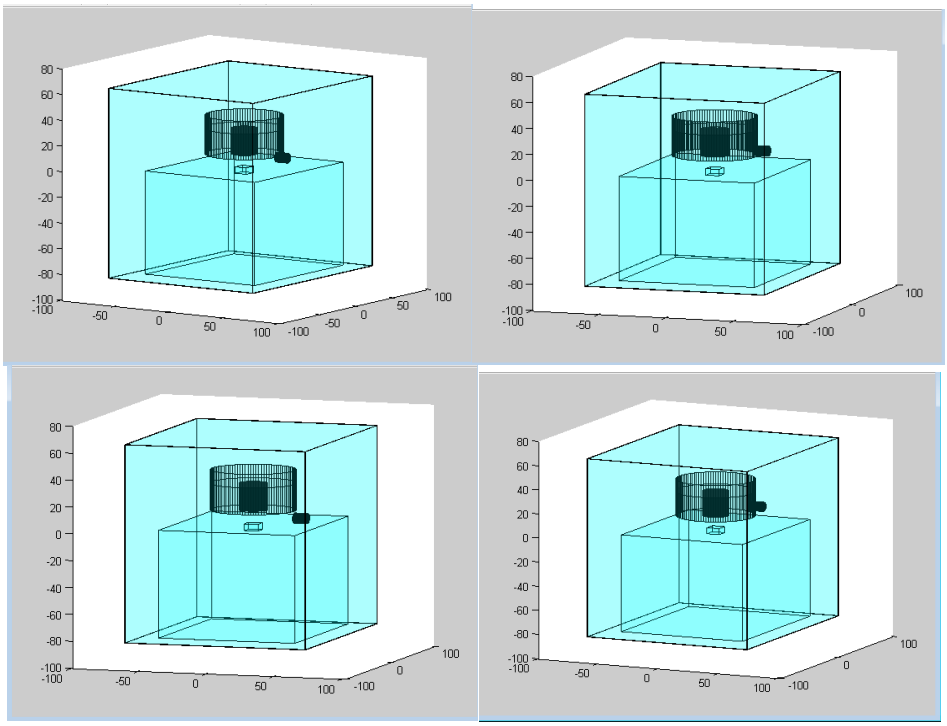

Fig. 15 The location of the $CeBr_3$ detector varies along the z-axis from 5 to 20 cm in increments of 5 cm

In the simulation, the melamine target is 5- × 5-cm^2 located 2.5-cm deep. The front of $CeBr_3$ is 30 cm away from the center of the melamine target in the horizontal direction. Shielding is 10 cm above soil. The $CeBr_3$ detector height is varied from 5 to 20 cm above soil in 5-cm increments.

Similar to the simulation limitation in Section 3.2, the simulation was unable to eliminate capture and absorption. The trajectory length of gammas increases as the detector height increases above the ground. We would expect that the pFlux should decrease via the inverse square law. The data for the gamma flux in the 5-cm detector height are less than that of the 10-cm detector height (Fig. 16). Trajectory lengths of 30.9 and 32.5 cm of the gammas were calculated (using the Pythagorean theorem) and the detector was 5 and 10 cm above soil, respectively.

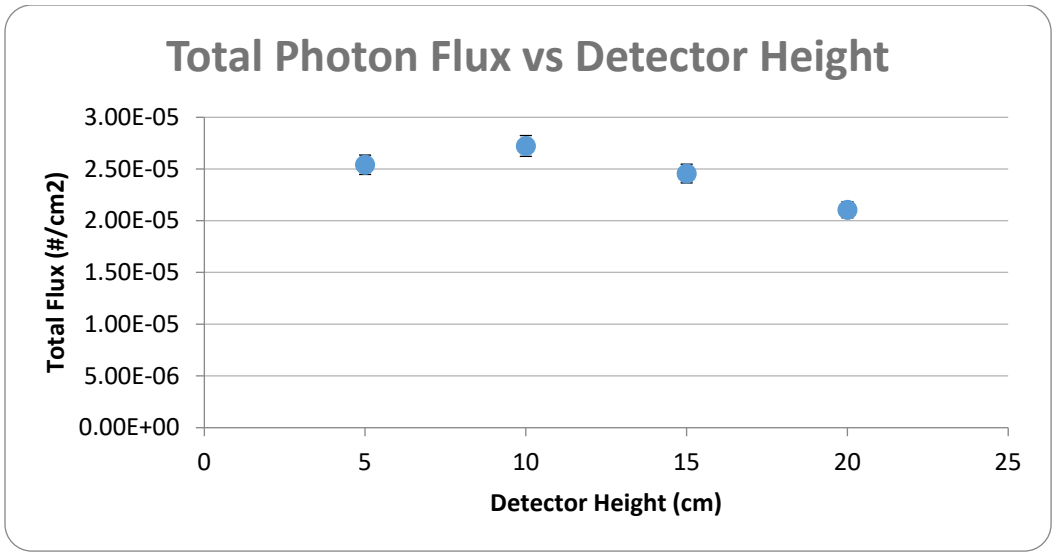

Fig. 16 Photon flux measured from gamma-sourced target volume is shown for $CeBr_3$ located at specified height above ground

There are three different attenuating materials in the gamma trajectory path. High-density polyethylene provides 1000 times greater attenuation to 10-MeV gammas than air, and soil provides 800 times greater attenuation to 10-MeV gammas than air. The tenth-value layer (TVL) thicknesses are shown in Fig. 17. Soil is the primary medium between the gamma source and the detector located 5-cm above, whereas air is the primary medium between the gamma source and the 10-cm detector. The trajectory difference between the 5- and 10-cm location is approximately 5%. The apparent angle is defined as the angle subtended by the isotropic gamma detector. These angles are shown in Fig. 18. The difference of approximately 2% was calculated in the apparent angle. Because the apparent angle of the 10-cm detector height is greater than the 5-cm location of the detector, the 10-cm detector naturally has more surface area to capture gammas. The combination of reduced apparent angle and TVL of the medium traversed appears to be the cause of increased gamma flux calculated at 10-cm height.

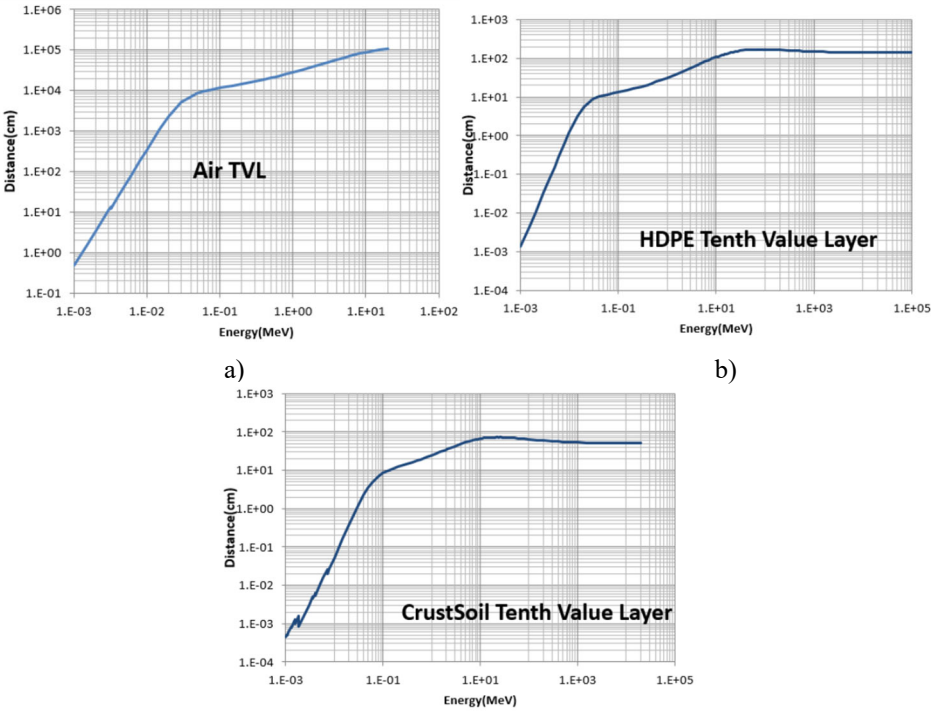

Fig. 17 TVL of a) air, b) HDPE, and c) soil[10]

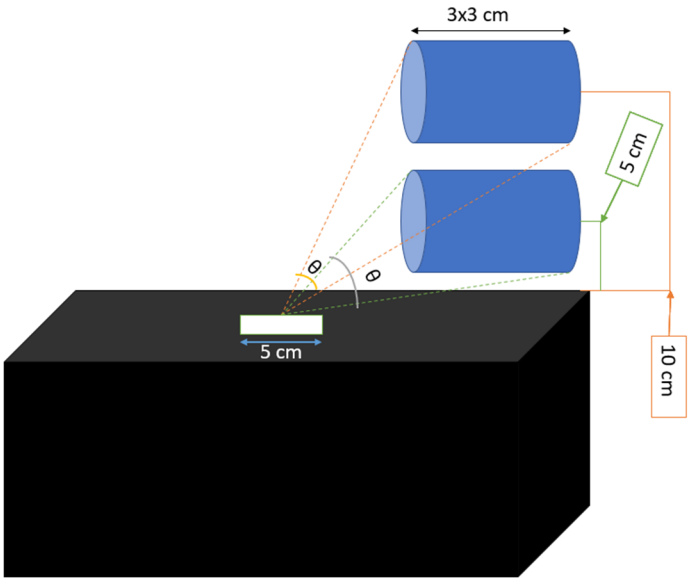

Fig. 18 Apparent (θ) angle calculation trajectories

3.4 Varying Shield and Detector Height

The goal of this simulation is to maximize pFlux, in $CeBr_3$, as HDPE shield height (along with detector height) is varied above ground. Every parameter in this simulation is the same as the parameters in Section 3.3 except that the shielding height is repositioned to be 0 cm above the soil. This series removes the air as a medium for the gammas. The $CeBr_3$ detector position (Fig. 19) varied from 5 to 15 cm above soil in 5-cm increments. The detector height could not be 20 cm because that area is around the cap of the shielding where photons cannot be detected (Appendix E for input deck).

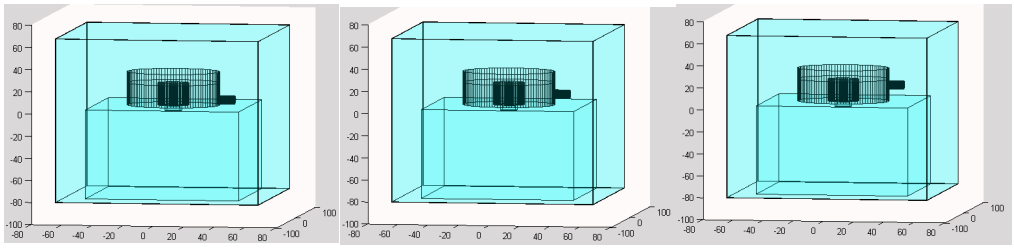

Fig. 19 The location of $CeBr_3$ detector varies along the z-axis from 5 to 20 cm in increments of 5 cm. Shield position is 0 cm above soil.

When the shield is directly on the ground and the air path component is eliminated from the calculation, the gamma flux in the detector reduces linearly. The parameter study in this section shows that when 10-cm air layer is removed, the gamma flux monotonically decreases (Fig. 20). This explains the 10-cm maximum gamma flux (anomaly) indicated in Section 3.3 (Fig. 16).

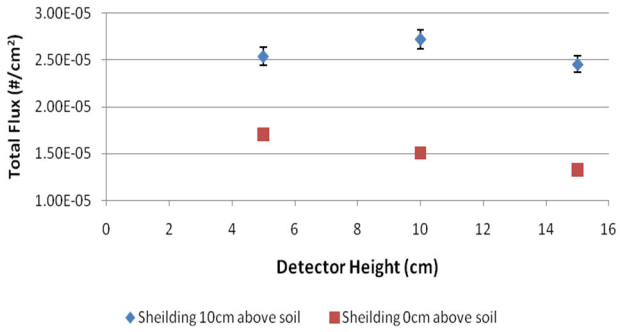

Fig. 20 Comparison of pFlux in $CeBr_3$ when HDPE shielding was 10 cm above soil and 0 cm above soil. Error bars in shielding 0 cm above soil is small and hidden by the plotter size.

3.5 Neutron Source Height Variation

As discussed in Sections 3.3 and 3.4, both the shielding and $CeBr_3$ detector 10 cm above soil maximizes the gamma flux in detector. The melamine target dimension is still the same as melamine target in Sections 3.3 and 3.4. A 2.5-MeV

isotropic neutron source height is varied between 11 and 19 cm above the ground. The neutron source is encapsulated in HDPE shield (Appendix F for input deck). Neutron source height was varied to find the optimal source height that results in maximized pFlux in $CeBr_3$ detector as well as maximized nFlux in target.

Figure 21 shows that as the source height is increased, both pFlux and nFlux decrease in $CeBr_3$ located 10 cm above the soil. As the neutron source height increases from 11 to 19 cm, the nFlux decreases 46% in the detector. As the neutron source height increases from 11 to 19 cm, the pFlux decreases 3.8% in the detector.

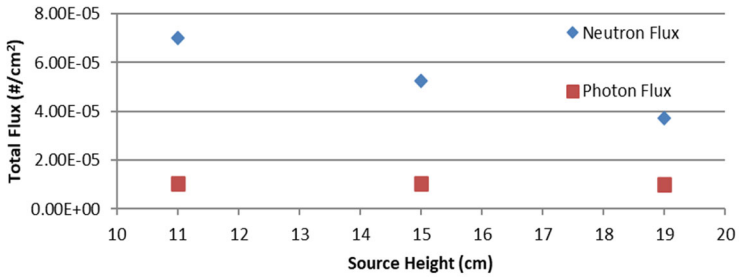

Fig. 21 Comparison of photon and nFlux in $CeBr_3$ for isotropic neutron source positioned at 11 and 19 cm above the soil. Error bars are hidden by plotting marker.

It is also ideal to maximize nFlux in the target. Greater nFlux in the target will generate the maximum amount of gamma rays for the detector. Figure 22 shows that between neutron source at the height of 11 and 19 cm, both nFlux and pFlux decrease by approximately 40%. The nFlux decreases 40% in the target correlates to a possible 40% decrease of pFlux in $CeBr_3$.

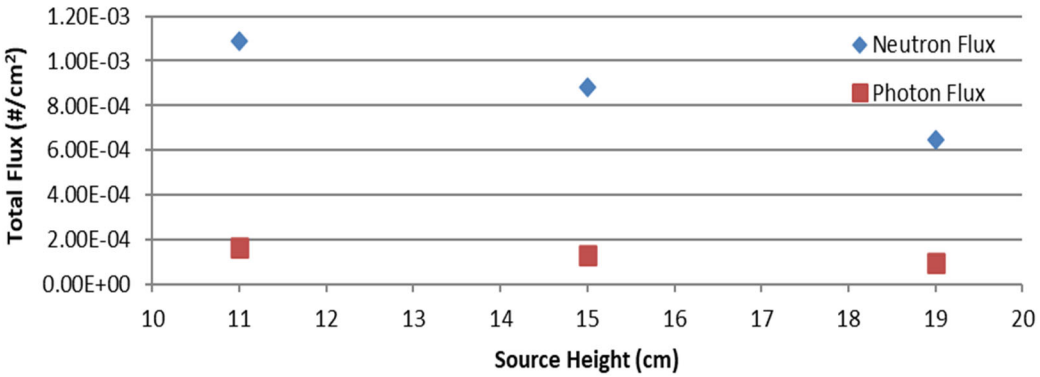

Fig. 22 Comparison of photon and nFlux in target for isotropic neutron source positioned at 11 and 19 cm above the soil. Error bars are hidden by plotting marker.

As stated in the introduction, boron shielding was used to reduce nFlux in the $CeBr_3$ detector. To observe the effects of boron shielding, a simulation was performed where the boron shield was changed to carbon shield. Figure 23 shows that carbon shielding increases nFlux in the detector by 41%. A significant decrease in the

pFlux is observed when boron shield is replaced with carbon shield (Fig. 24). Although boron shielding reduces nFlux in the detector, it also increases 0.478-MeV gammas in the detector, which are not gammas of interest. It is unclear why there is a dip in the nFlux at 15 cm.

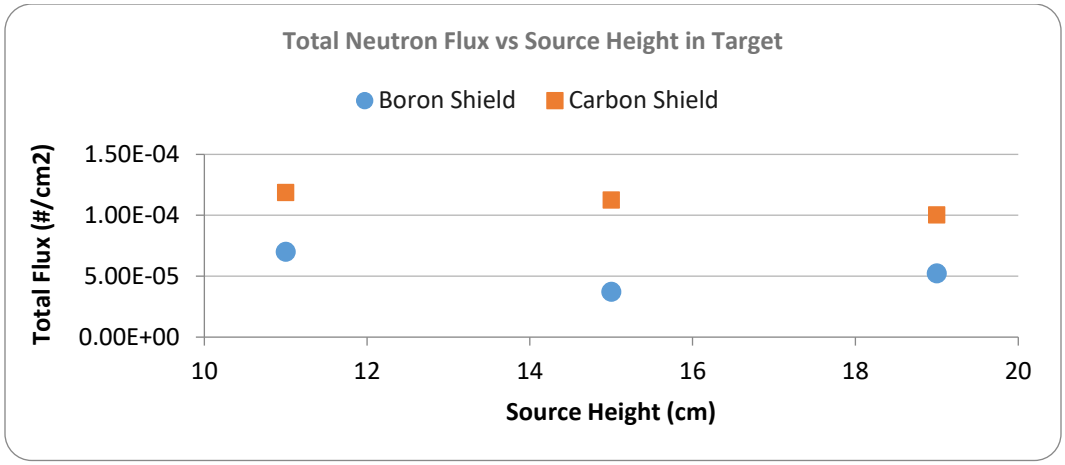

Fig. 23 Comparison of nFlux with boron and carbon shielding in $CeBr_3$ for isotropic neutron source positioned at 11 and 19 cm above the soil. Error bars are hidden by plotting marker.

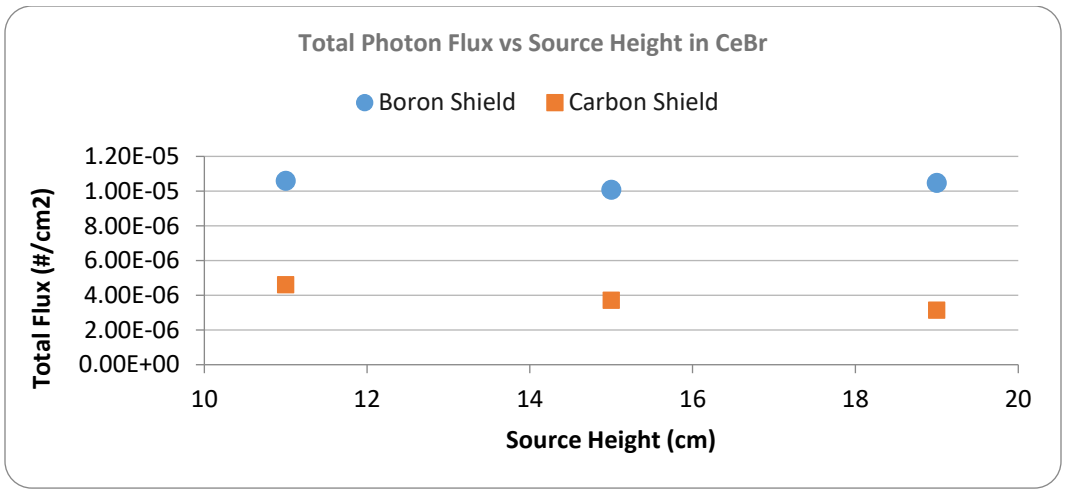

Fig. 24 Comparison of pFlux with boron and carbon shielding in $CeBr_3$ for isotropic neutron source positioned at 11 and 19 cm above the soil. Error bars are hidden by plotting marker.

Another simulation was run without soil, just air, to account for the neutron reflection from the soil, neutrons that are scattered from soil. By replacing soil with air, the neutrons will have no medium to scatter off, hence providing data only produced from target. Figure 25 shows that the reflected neutrons are a large contributor in creating nFlux in the detector. By taking the ratio of total nFlux in soil and air simulation, an approximately 79% to 81% increase in nFlux in soil simulation is observed. This result implies that most of nFlux in the detector is from soil reflection. This result implies that better shielding is needed to prevent the reflected neutrons from being detected in the $CeBr_3$ detector.

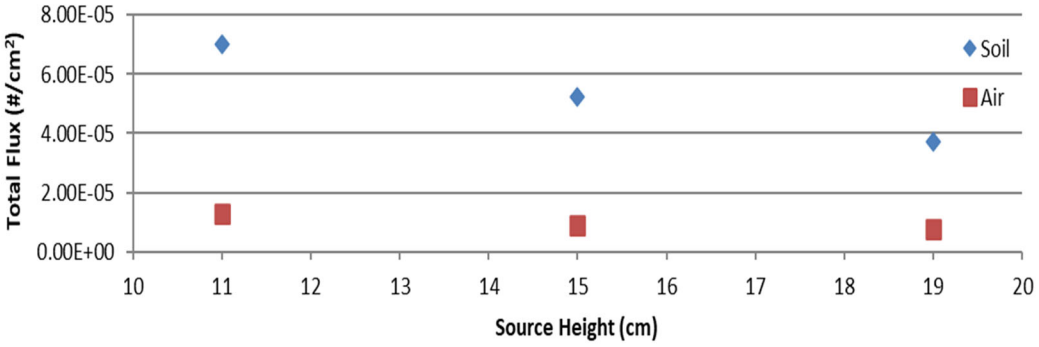

Fig. 25 Neutron flux in $CeBr_3$ measured from an isotropic neutron source positioned at 11, 15, and 19 cm. Approximately 79%–81% are reflected neutrons. Error bars are hidden by plotting marker.

4. Discussion of Gamma Analysis

Parameter optimizations in MCNP simulations were conducted to detect detailed gamma spectrum in the $CeBr_3$ detector. The soil content in the simulations contained trace elements of the following: Ni, Cr, O, Si, Al, Fe, Ca, Na, B, N, and Ar. When neutrons interact with these nuclei, one of the possible reactions is thermal neutron capture, which often produces characteristic gamma rays. Inelastic and elastic scattering reactions are also possible. Using all the optimized parameters from Section 3, a 950-M history MCNP run was conducted (100-M histories took 7.2 h on a standard PC). Figure 26 shows all expected elemental soil lines were observed. From Fig. 26, observing flux of 0.478-MeV gamma and 10.8 MeV, the detector will detect approximately 1 in 300,000 0.478-MeV gamma and 1 in 30 billion 10.8-MeV gammas per sourced neutron. This shows that the detector is about 100,000 times more efficient in detecting 0.478-MeV gammas than 10-MeV gammas.

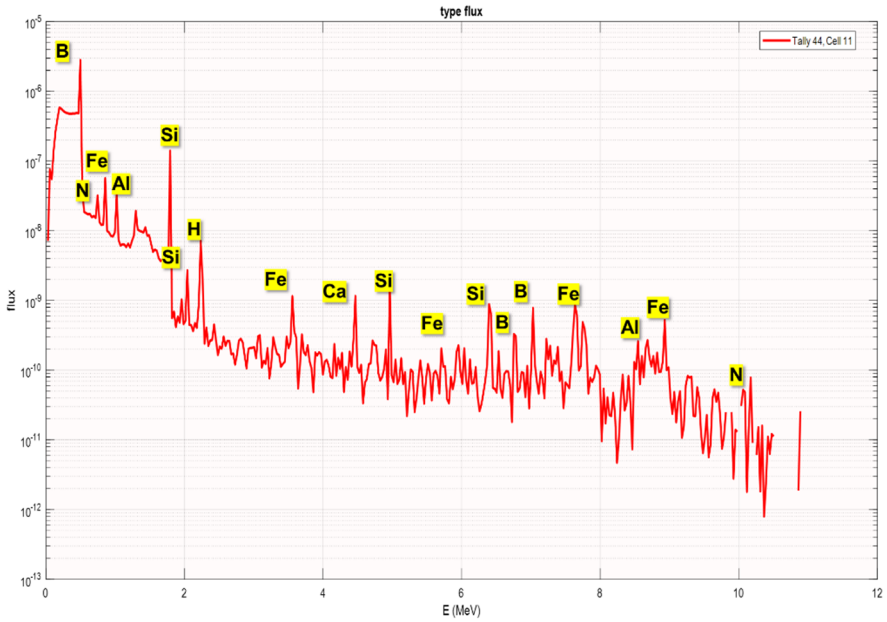

Fig. 26 Gamma spectra shown in detector cell 11 (red) with resolution of 27.5 keV

The statistic of the simulation is also important in determining the validity of the data. Figure 27 shows that the relative error (R) (Eq. 4) of the simulation is valid for gamma up to 2.1 MeV. Beyond 2.1 MeV, the results in Fig. 27 show a high signal-to-noise ratio.

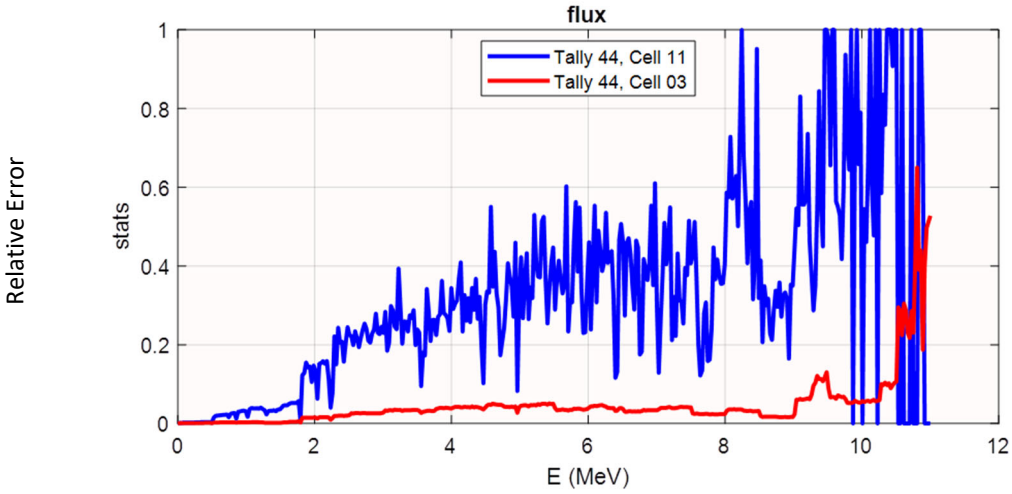

Fig. 27 Relative error in gamma spectra shown in target, cell 3 (red), and in detector cell 11 (blue)

Figure 28 depicts a semi-log plot of the gamma flux (lines identified in Fig. 26) with error bars included as calculated using Eq. 4. The error bars are primarily correlated to the FOM shown in Fig. 27. Figure 28 shows a relatively small error bar, in peaks of interest, which implies that simulation statistics are valid at gamma energies where counts are occurring.

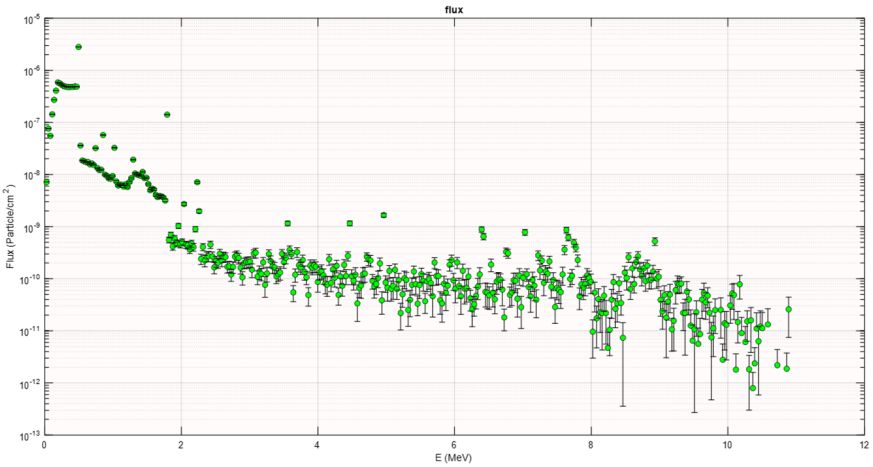

Fig. 28 Neutron-sourced gamma spectrum in $CeBr_3$ with error bar

5. Conclusion

In the first set of variations, HDPE shield radius around source varied from 10 to 35 cm. The nFlux in the $CeBr_3$ dropped 90% when HDPE radius was varied from 10 to 30 cm. When the simulation included a layer of soil under the neutron source, shield, and detector combination, the neutron flux in the $CeBr_3$ dropped 62% when the HDPE radius was varied from 10 to 30 cm. The soil reflection was generating 38% more nFlux in $CeBr_3$. In the second parameter study, the 125-cc melamine target depth varied from 2.5 to 57.5 cm. The total nFlux dropped by a factor of 10 over this range. The thermal nFlux decreased linearly with distance in the soil, whereas the 2.5-MeV flux decreased exponentially with depth in soil. In the third parameter study, the $CeBr_3$ detector was varied 5 to 10 cm above ground. In the fourth parameter study, the fluxes were compared for HDPE heights of 0 cm and 10 cm above the ground. The gamma flux in $CeBr_3$ detector was maximized when the detector and the HDPE shield were located 10 cm above the ground. In the fifth parameter study, the isotropic neutron source was varied between 11 and 19 cm. Raising the neutron source from 11 to 19 cm above the ground reduces the nFlux in the target by 40%. Raising the neutron source from 11 to 19 cm above the ground reduces the nFlux in the $CeBr_3$ detector by 46%. With all these optimized positions, gamma spectrum was calculated using 100 Mh to get statistically valid results.

6. Path Forward

As discussed in Section 4, the $CeBr_3$ detector will detect 1 in 30 billion high-energy gammas, which would not be problematic if the detector is collecting data for a longer period, like NASA's LEND instrument. However, for earth-based operations that detect explosives in ground, fast data collection is ideal. With the current geometry, $CeBr_3$ is insufficient in detecting high-energy gammas. From Fig. 27, we suspect that much of the high-energy gammas deposit partial energy into the detector. Because of this reason, it would be ideal to run simulations with multiple detectors in different geometrical orientations to catch scattered gammas. By adding all the scattered gamma, in the exact time range, it may be possible to account for all the high-energy gammas coming off the soil, which will then lessen the time required to detect high-energy gammas. Statistical tension within the simulation provides noise in the data. In the future, it would be ideal to run a larger number of histories in MCNP. The less noise there is in the data, the easier it is to identify the efficiency of the detector.

7. References

1. Litz M, Waits C, Mullins J. Neutron-activated gamma-emission: technology review. Army Research Laboratory (US): 2012 Jan. Report No.: ARL-TR-5871.

2. Shen W, Rouben B. Neutrons and neutron interactions. In: Fundamentals of CANDU reactor physics. American Society of Mechanical Engineers Press; 2021. Essay. p. 43–49.

3. Prettyman TH, Hagerty JJ, Elphic RC, Feldman WC, Lawrence DJ, McKinney GW, Vaniman DT. Elemental composition of the lunar surface: analysis of gamma ray spectroscopy data from Lunar Prospector. J Geophys Res. 2006;111:E12007. doi:10.1029/2005JE002656.

4. Litvak ML, Mitrofanov IG, Sanin A, Malakhov A, Boynton WV, Chin G, Droege G, Evans LG, Garvin J, Golovin DV, et al. Global maps of lunar neutron fluxes from the LEND instrument. J Geophys Res. 2012;117:E00H22. doi:10.1029/2011JE003949.

5. Yasin T, Khan MN. High density polyethylene/boron carbide composites for neutron shielding. E-Polymers. 2008;8(1):059. https://doi.org/10.1515/epoly.2008.8.1.670.

6. nuclear-power.com. Boron 10. Nuclear-power.com; 17 Oct 2021 [accessed 2022 Sep 12]. https://www.nuclear-power.com/glossary/boron-10/.

7. Shultis JK, Faw RE. An MCNP primer. Kansas State University, Department of Mechanical and Nuclear Engineering; 2011.

8. Pelowitz D, Fallgren A, Mcmath G. MCNP6 user's manual, version 6.1.1beta. Los Alamos National Laboratory (US); 2014 June. Report No.: LA-CP-14-00745.

9. Kulesza JA, Adams TR, Armstrong JC, Bolding SR, Brown FB, Bull JS, Burke TP, Clark AR, Forster RA III, Giron JF, et al. MCNP code version 6.3.0 theory & user manual. Los Alamos National Laboratory (US); 2022 Sep. Report No.: LA-UR-22-30006.

10. Hubbell JH, Seltzer SM. X-ray mass attenuation coefficients. NIST; 2022 Feb 17 [accessed 2022 Sep 12]. https://www.nist.gov/pml/x-ray-mass-attenuation-coefficients.

Appendix A. MCNP Input Deck for Section 3.1

This appendix appears in its original form, without editorial change.

The following is an example MCNP input deck for Section 3.1.

```
Model of 30%B HDPE 10cm rad C
c
c target in air
c 6” cube (next time cubesat)
c DD 27eutron source
c Edited by Ryan Brockington
c
c +-------------------------------------------------+
c |                                                 |
c |                  Cell Cards                     |
c |                                                 |
c +-------------------------------------------------+
c # mat   density   surface        data
c
 3  1   -7.7       -3  imp:n,e,p 1 u=1   $Melamin block
52  16   -1.47     -52 3   imp:n,e,p 1 u=1  $ground base
 7  3    -2.3       -7    imp:n,e,p 1 u=1      $ vault
 8  6   -0.918      -8 18  imp:n,e,p 1 u=1     $ vault
18  3   -2.3        -18 9  imp:n,e,p 1 u=1     $ vault
 9  2   -0.00129  -9    imp:n,e,p 1 u=1        $air cavity
11  5   -5.06     -11    imp:n,e,p 1 u=1    $CeBr0
c 12  4   -11.3     -12    imp:n,e,p 1 u=1      $ extra Pb for CeBr
c air encasing
 31  2    -0.00129   -31  3 52 7 8 9 11   imp:n,e,p 1  u=1
 32  0     31                    imp:n,e,p 1  u=1
c room
 34  2    -0.00129   -32   imp:n,e,p 1 fill=1
 35  0               32   imp:n,e,p 0        $outside world
```

```
c +--------------------------------------------------+
c |                                                  |
c |                  Surface Cards                   |
c |                                                  |
c +--------------------------------------------------+
c # type params
c
 3   rpp  -5 5   -5 5     -5   0      $Melamin/TNT/DUT
 52  rpp  -50 50  -60 60  -80   0    $air/ground base
 7   rcc  0 0 30   0 0 10  30       $vault top   25cm shield
 8   rcc  0 0 10   0 0 20  30       $vault box   25cm shield
 18   rcc  0 0 10   0 0 20  10      $vault carbon   25cm shield
 9   rcc   0 0 10   0 0 20  2.5      $air/space inside vault
 11  rcc   30 0 10   10 0 0  3.81  $CeBr
c air background
31   rpp  -66 66      -86 76      -81 66
c room dimensions
32   rpp  -66.2 66.2  -86.2 76.2  -81.2 66.2


c +--------------------------------------------------+
c |                                                  |
c |                  Material Cards                  |
c |                                                  |
c +--------------------------------------------------+
c m# isotope    percent           $comment
 m2   6000       0.000150      $air 0.00129 g/cc
      7014       0.784431
      8016       0.210748
      18000      0.004671
```

```
m4   82000      1.0          $lead 11.34 g/cc
m1   28000      0.8          $NiCr 7.7 g/cc
     24000      0.2
m3   6012       1.0          $C   2.3 g/cc
m6   5010.70c   0.33         $BPE  bc2h4  0.918 g/cc
     6012       0.22
     1001.24    0.44
m5   58140.70c  0.25         $CeBr3  5.06 g/cc
     35079.70c  0.75
m16  8016       0.670604     $soil, U.S. Avg  1.47  O Si Al Fe Ca Na
     11023      0.005578
     12000      0.011432
     13027      0.053073
     14000      0.201665
     19000      0.007653
     20000      0.026664
     22000      0.002009
     25055      0.000272
     26000      0.021050
c
c +-------------------------------------------------+
c |                                                 |
c |                  Source Definition              |
c |                                                 |
c +-------------------------------------------------+
 sdef par=n  pos=0 0 19 erg=2.5
si1 0 1
sp1 -21
c
c +-------------------------------------------------+
```

```
c |                                                    |
c |                  Data Cards                        |
c |                                                    |
c +----------------------------------------------------+
mode n p e
  PHYS:E 100 0 0 0 0 1 1 1 1 0
c  PHYS:N 100 0 0 -101 -1 0 0
  PHYS:N
c  PHYS:P 100 0 0 0 1 -101
  PHYS:P
  cut:n j j 0 0
  cut:p j j 0 0 4
ptrac nps=1,1000 type=n file=asc event=bnk,sur,col,ter,cap
nps 68000000     $ 1M-1.8min originally 5000000
c
c +----------------------------------------------------+
c |                                                    |
c |                  Tallies                           |
c |                                                    |
c +----------------------------------------------------+
c
c fc5 gamma variance reduction
c   f5:p  50 -5 10   .3
c   e5 0 398i 11
fc14 neutron flux
  f14:n  11 3
  e14 .00001 398log 3
fc24 neutron flux
  f24:n  11 3
  e24 0 398i 3
```

```
fc34 neutron flux
 f34:n  52
 e34 .000001 398log .01
fc44 photon flux
 f44:p  11 3
 e44 0 398i 11
fc16 neutron Edep averaged over the cell in MeV/g
 f16:n  11 3
 e16 0 398i 3
fc26 photon Edep averaged over the cell in MeV/g
 f26:p  11  3
 e26 0 398i 11
c
c +-----------------------------------------------------+
c |                                                     |
c |                    Mesh                             |
c |                                                     |
c +-----------------------------------------------------+
c
tmesh
c
c (a)radial meshes (b)zaxis(symmetry) (c)angles counterclockwise
c
c  flux=#/cm2     $dose=rem/hr    $pedep=MeV/cm3
c
c flux: flux
c pedep: total energy deposition/unit vol
c dose: dose over cross planes
c
rmesh1:n  flux pedep
```

```
c first layer area
cora1    -60  98i  60
corb1    -70  138i 70
corc1    -90       60
c
rmesh31:n  flux pedep
c first layer area
cora31    -60        60
corb31    -70   98i  70
corc31    -90  138i  60
c
rmesh21:n  flux pedep
c first layer area
cora21    -60  138i  60
corb21    -70        70
corc21    -90   98i  60
c
rmesh41:p  flux pedep
c first layer area
cora41    -60  138i  60
corb41    -70        70
corc41    -90   98i  60
c
endmd
```

Appendix B. MCNP Input Deck for Section 3.2

This appendix appears in its original form, without editorial change.

The following is an example MCNP input deck for Section 3.22

```
Model of 30% B HDPE 10-cm rad C
c
c target in air
c 6” cube (next time cubesat)
c DD 34eutron source
c Edited by Ryan Brockington
c
c +-----------------------------------------------------+
c |                                                     |
c |                    Cell Cards                       |
c |                                                     |
c +-----------------------------------------------------+
c # mat   density   surface        data
c
 3  1   -7.7       -3  imp:n,e,p 1 u=1   $Melamin block
52  16   -1.47     -52 3   imp:n,e,p 1 u=1  $ground base
 7  3    -2.3       -7    imp:n,e,p 1 u=1      $ vault
 8  6   -0.918      -8 18  imp:n,e,p 1 u=1     $ vault
18  3   -2.3        -18 9  imp:n,e,p 1 u=1     $ vault
 9  2   -0.00129  -9    imp:n,e,p 1 u=1        $air cavity
11  5   -5.06     -11    imp:n,e,p 1 u=1    $CeBr0
c air encasing
 31  2    -0.00129   -31  3 52 7 8 9 11   imp:n,e,p 1  u=1
 32  0     31                    imp:n,e,p 1  u=1
c room
 34  2    -0.00129   -32   imp:n,e,p 1 fill=1
 35  0               32   imp:n,e,p 0        $outside world
```

```
c +--------------------------------------------------+
c |                                                  |
c |                  Surface Cards                   |
c |                                                  |
c +--------------------------------------------------+
c # type params
c
 3   rpp  -5 5   -5 5     -5   0      $Melamin/TNT/DUT
 52  rpp  -50 50  -60 60  -42.99   0    $air/ground base
 7   rcc  0 0 30   0 0 10  30       $vault top   25cm shield
  8   rcc  0 0 10   0 0 20  30      $vault box   25cm shield
 18   rcc  0 0 10   0 0 20  10      $vault carbon   25cm shield
 9   rcc   0 0 10   0 0 20  2.5       $air/space inside vault
 11  rcc   35 -10 10   0 10 0    5  $CeBr
c air background
31   rpp  -66 66      -86 76      -81 66
c room dimensions
32   rpp  -66.2 66.2  -86.2 76.2  -81.2 66.2


c +--------------------------------------------------+
c |                                                  |
c |                 Material Cards                   |
c |                                                  |
c +--------------------------------------------------+
c m# isotope    percent           $comment
 m2   6000       0.000150      $air 0.00129 g/cc
      7014       0.784431
      8016       0.210748
      18000      0.004671
 m4   82000      1.0          $lead 11.34 g/cc
```

```
m1   28000      0.8          $NiCr 7.7 g/cc
     24000      0.2
m3   6012       1.0          $C   2.3 g/cc
m6   5010.70c   0.33         $BPE  bc2h4  0.918 g/cc
     6012       0.22
     1001.24    0.44
m5   58140.70c  0.25         $CeBr3  5.06 g/cc
     35079.70c  0.75
m16  8016       0.670604     $soil, U.S. Avg  1.47  O Si Al Fe Ca Na
     11023      0.005578
     12000      0.011432
     13027      0.053073
     14000      0.201665
     19000      0.007653
     20000      0.026664
     22000      0.002009
     25055      0.000272
     26000      0.021050
c
c +-----------------------------------------------------+
c |                                                     |
c |                  Source Definition                  |
c |                                                     |
c +-----------------------------------------------------+
 sdef par=n  pos=0 0 20 erg=2.5
c  &           vec=0 0 -1  dir=1  rad=d1
 si1 0 1
 sp1 -21
c
c +-----------------------------------------------------+
```

```
c |                                                    |
c |                  Data Cards                        |
c |                                                    |
c +----------------------------------------------------+
mode n p e
  PHYS:E 100 0 0 0 0 1 1 1 1 0
c  PHYS:N 100 0 0 -101 -1 0 0
  PHYS:N
c  PHYS:P 100 0 0 0 1 -101
  PHYS:P
  cut:n j j 0 0
  cut:p j j 0 0 4
ptrac nps=1,1000 type=n file=asc event=bnk,sur,col,ter,cap
nps 3000000     $ 1M-1.8min originally 5000000
c
c +----------------------------------------------------+
c |                                                    |
c |                  Tallies                           |
c |                                                    |
c +----------------------------------------------------+
c
fc14 neutron flux
  f14:n  11 3
  e14 .00001 398log 3
fc24 neutron flux
  f24:n  11 3
  e24 0 398i 3
fc34 neutron flux
  f34:n  52
  e34 .000001 398log .01
```

```
fc44 photon flux
 f44:p  11 3
 e44 0 398i 11
fc16 neutron Edep averaged over the cell in MeV/g
 f16:n  11 3
 e16 0 398i 3
fc26 photon Edep averaged over the cell in MeV/g
 f26:p  11  3
 e26 0 398i 11
c
c +-----------------------------------------------------+
c |                                                     |
c |                    Mesh                             |
c |                                                     |
c +-----------------------------------------------------+
c
tmesh
c
c (a)radial meshes (b)zaxis(symmetry) (c)angles counterclockwise
c
c  flux=#/cm2     $dose=rem/hr    $pedep=MeV/cm3
c
c flux: flux
c pedep: total energy deposition/unit vol
c dose: dose over cross planes
c
rmesh1:n  flux pedep
c first layer area
cora1    -60  98i  60
corb1    -70  138i 70
```

```
corc1    -40       60
c
rmesh31:n  flux pedep
c first layer area
cora31    -60        60
corb31    -70   98i  70
corc31    -40  138i  60
c
rmesh21:n  flux pedep
c first layer area
cora21    -60  138i  60
corb21    -70        70
corc21    -40   98i  60
c
rmesh41:p  flux pedep
c first layer area
cora41    -60  138i  60
corb41    -70        70
corc41    -40   98i  60
c
endmd
```

Appendix C. MCNP Input Deck for Section 3.3

This appendix appears in its original form, without editorial change.

The following is an example MCNP input deck for Section 3.3.

```
Model of 30% B HDPE 10-cm rad C
c
c target in air
c 6” cube (next time cubesat)
c DD 41eutron source
c Edited by Ryan Brockington
c
c +--------------------------------------------------+
c |                                                  |
c |                  Cell Cards                      |
c |                                                  |
c +--------------------------------------------------+
c # mat   density   surface       data
c
 3  1   -7.7      -3      imp:n,e,p 1 u=1   $Melamin block
52  16  -1.47     -52 3   imp:n,e,p 1 u=1   $ground base
 7  3   -2.3      -7      imp:n,e,p 1 u=1   $ vault
 8  6   -0.918    -8  18  imp:n,e,p 1 u=1   $ vault
18  3   -2.3      -18 9   imp:n,e,p 1 u=1   $ vault
 9  2   -0.00129  -9      imp:n,e,p 1 u=1   $air cavity
11  5   -5.06     -11     imp:n,e,p 1 u=1   $CeBr0
c air encasing
31  2   -0.00129  -31 3 52 7 8 9 11   imp:n,e,p 1  u=1
32  0    31                          imp:n,e,p 1  u=1
c room
34  2   -0.00129  -32     imp:n,e,p 1 fill=1
35  0             32      imp:n,e,p 0       $outside world


c +--------------------------------------------------+
```

```
c |                                                    |
c |                    Surface Cards                   |
c |                                                    |
c +----------------------------------------------------+
c # type params
c
 3   rpp  -5  5   -5  5   -5    0    $Melamin/TNT/DUT
 52  rpp  -50 50  -60 60  -80   0    $air/ground base
 7   rcc  0 0 30   0 0 10  30        $vault top   25cm shield
 8   rcc  0 0 10   0 0 20  30        $vault box   25cm shield
 18  rcc  0 0 10   0 0 20  10        $vault carbon   25cm shield
 9   rcc  0 0 10   0 0 20  2.5       $air/space inside vault
 11  rcc  30 0 10   10 0 0  3.81       $CeBr
c air background
31   rpp  -66 66      -86 76      -81 66
c room dimensions
32   rpp  -66.2 66.2  -86.2 76.2  -81.2 66.2


c +----------------------------------------------------+
c |                                                    |
c |                   Material Cards                   |
c |                                                    |
c +----------------------------------------------------+
c m# isotope    percent           $comment
 m2   6000       0.000150      $air 0.00129 g/cc
      7014       0.784431
      8016       0.210748
      18000      0.004671
 m4   82000      1.0           $lead 11.34 g/cc
 m1   28000      0.8           $NiCr 7.7 g/cc
```

```
     24000      0.2
 m3   6012       1.0          $C   2.3 g/cc
 m6   5010.70c   0.33         $BPE  bc2h4  0.918 g/cc
     6012       0.22
     1001.24    0.44
 m5   58140.70c  0.25         $CeBr3  5.06 g/cc
     35079.70c  0.75
 m16  8016       0.670604     $soil, U.S. Avg  1.47  O Si Al Fe Ca Na
     11023      0.005578
     12000      0.011432
     13027      0.053073
     14000      0.201665
     19000      0.007653
     20000      0.026664
     22000      0.002009
     25055      0.000272
     26000      0.021050
c
c +-----------------------------------------------------+
c |                                                     |
c |                  Source Definition                  |
c |                                                     |
c +-----------------------------------------------------+
 sdef par=p  pos=0 0 -2.5 erg=D1
SI1 L 0.478 2.223 3.540 4.432 7.100 10.800
SP1   1 1 1 1 1 1
c  si3 h .707 1
c  sp3 d 0 1
c
c +-----------------------------------------------------+
```

```
c |                                                    |
c |                    Data Cards                      |
c |                                                    |
c +----------------------------------------------------+
mode n p e
  PHYS:E 100 0 0 0 0 1 1 1 1 0
c  PHYS:N 100 0 0 -101 -1 0 0
  PHYS:N
c  PHYS:P 100 0 0 0 1 -101
  PHYS:P
  cut:n j j 0 0
  cut:p j j 0 0 4
nps 500000     $ 1M-1.8min originally 5000000
c
c +----------------------------------------------------+
c |                                                    |
c |                     Tallies                        |
c |                                                    |
c +----------------------------------------------------+
c
fc44 photon flux
  f44:p  11 3
  e44 0 398i 11
c fc16 neutron Edep averaged over the cell in MeV/g
c  f16:n  11 3
c  e16 0 398i 3
fc26 photon Edep averaged over the cell in MeV/g
 f26:p  11  3
 e26 0 398i 11
c
```

```
c +--------------------------------------------------+
c |                                                  |
c |                    Mesh                          |
c |                                                  |
c +--------------------------------------------------+
c
tmesh
c
c (a)radial meshes (b)zaxis(symmetry) (c)angles counterclockwise
c
c  flux=#/cm2     $dose=rem/hr    $pedep=MeV/cm3
c
c flux: flux
c pedep: total energy deposition/unit vol
c dose: dose over cross planes
c
rmesh1:n  flux pedep
c first layer area
cora1    -60  98i  60
corb1    -70  138i 70
corc1    -90       60
c
rmesh31:n  flux pedep
c first layer area
cora31    -60        60
corb31    -70   98i  70
corc31    -90  138i  60
c
rmesh21:n  flux pedep
c first layer area
```

```
cora21    -60  138i  60
corb21    -70        70
corc21    -90   98i  60
c
rmesh41:p  flux pedep
c first layer area
cora41    -60  138i  60
corb41    -70        70
corc41    -90   98i  60
c
endmd
```

Appendix D. MCNP Input Deck for Section 3.4

This appendix appears in its original form, without editorial change.

The following is an example MCNP input deck for Section 3.4.

```
Model of 30% B HDPE 10-cm rad C
c
c target in air
c 6” cube (next time cubesat)
c DD 48eutron source
c Edited by Ryan Brockington
c
c +-------------------------------------------------+
c |                                                 |
c |                  Cell Cards                     |
c |                                                 |
c +-------------------------------------------------+
c # mat   density   surface       data
c
 3  1   -7.7       -3  imp:n,e,p 1 u=1   $Melamin block
52  16   -1.47     -52 3   imp:n,e,p 1 u=1  $ground base
 7  3    -2.3       -7    imp:n,e,p 1 u=1      $ vault
 8  6   -0.918      -8 18  imp:n,e,p 1 u=1     $ vault
18  3   -2.3        -18 9  imp:n,e,p 1 u=1     $ vault
 9  2   -0.00129  -9    imp:n,e,p 1 u=1        $air cavity
11  5   -5.06     -11    imp:n,e,p 1 u=1    $CeBr0
c air encasing
 31  2    -0.00129   -31  3 52 7 8 9 11   imp:n,e,p 1  u=1
 32  0     31                    imp:n,e,p 1  u=1
c room
 34  2    -0.00129   -32   imp:n,e,p 1 fill=1
 35  0               32   imp:n,e,p 0        $outside world


c +-------------------------------------------------+
```

```
c |                                                      |
c |                    Surface Cards                     |
c |                                                      |
c +------------------------------------------------------+
c # type params
c
 3   rpp  -5 5   -5 5     -5   0      $Melamin/TNT/DUT
 52  rpp  -50 50  -60 60  -80   0    $air/ground base
 7   rcc  0 0 20   0 0 10  30       $vault top   25cm shield
  8   rcc  0 0 0   0 0 20  30      $vault box   25cm shield
 18   rcc  0 0 0   0 0 20  10      $vault carbon   25cm shield
 9   rcc   0 0 0   0 0 20  2.5       $air/space inside vault
 11  rcc  30 0 10   10 0 0  3.81       $CeBr
c air background
31   rpp  -66 66      -86 76      -81 66
c room dimensions
32   rpp  -66.2 66.2  -86.2 76.2  -81.2 66.2


c +------------------------------------------------------+
c |                                                      |
c |                   Material Cards                     |
c |                                                      |
c +------------------------------------------------------+
c m# isotope    percent           $comment
 m2   6000       0.000150      $air 0.00129 g/cc
      7014       0.784431
      8016       0.210748
      18000      0.004671
 m4   82000      1.0           $lead 11.34 g/cc
 m1   28000      0.8           $NiCr 7.7 g/cc
```

```
     24000      0.2
 m3   6012       1.0          $C   2.3 g/cc
 m6   5010.70c   0.33         $BPE  bc2h4  0.918 g/cc
     6012       0.22
     1001.24    0.44
 m5   58140.70c  0.25         $CeBr3  5.06 g/cc
     35079.70c  0.75
 m16  8016       0.670604     $soil, U.S. Avg  1.47  O Si Al Fe Ca Na
     11023      0.005578
     12000      0.011432
     13027      0.053073
     14000      0.201665
     19000      0.007653
     20000      0.026664
     22000      0.002009
     25055      0.000272
     26000      0.021050
c
c +-----------------------------------------------------+
c |                                                     |
c |                  Source Definition                  |
c |                                                     |
c +-----------------------------------------------------+
 sdef par=p  pos=0 0 -2.5 erg=D1
SI1 L 0.478 2.223 3.540 4.432 7.100 10.800
SP1   1 1 1 1 1 1
c
c +-----------------------------------------------------+
c |                                                     |
c |                  Data Cards                         |
```

```
c |                                                  |
c +--------------------------------------------------+
mode n p e
  PHYS:E 100 0 0 0 0 1 1 1 1 0
c  PHYS:N 100 0 0 -101 -1 0 0
  PHYS:N
c  PHYS:P 100 0 0 0 1 -101
  PHYS:P
  cut:n j j 0 0
  cut:p j j 0 0 4
ptrac nps=1,1000 type=n file=asc event=bnk,sur,col,ter,cap
nps 1800000     $ 1M-1.8min originally 5000000
c
c +--------------------------------------------------+
c |                                                  |
c |                    Tallies                       |
c |                                                  |
c +--------------------------------------------------+
c
fc14 neutron flux
  f14:n  11 3
  e14 .00001 398log 3
fc24 neutron flux
  f24:n  11 3
  e24 0 398i 3
fc34 neutron flux
  f34:n  52
  e34 .000001 398log .01
fc44 photon flux
  f44:p  11 3
```

```
 e44 0 398i 11
fc16 neutron Edep averaged over the cell in MeV/g
 f16:n  11 3
 e16 0 398i 3
fc26 photon Edep averaged over the cell in MeV/g
 f26:p  11  3
 e26 0 398i 11
c
c +--------------------------------------------------+
c |                                                  |
c |                  Mesh                            |
c |                                                  |
c +--------------------------------------------------+
c
tmesh
c
c (a)radial meshes (b)zaxis(symmetry) (c)angles counterclockwise
c
c  flux=#/cm2     $dose=rem/hr    $pedep=MeV/cm3
c
c flux: flux
c pedep: total energy deposition/unit vol
c dose: dose over cross planes
c
rmesh1:n  flux pedep
c first layer area
cora1    -60  98i  60
corb1    -70  138i 70
corc1    -90       60
c
```

```
rmesh31:n  flux pedep
c first layer area
cora31    -60        60
corb31    -70   98i  70
corc31    -90  138i  60
c
rmesh21:n  flux pedep
c first layer area
cora21    -60  138i  60
corb21    -70        70
corc21    -90   98i  60
c
rmesh41:p  flux pedep
c first layer area
cora41    -60  138i  60
corb41    -70        70
corc41    -90   98i  60
c
endmd
```

Appendix E. MCNP Input Deck for Section 3.5

This appendix appears in its original form, without editorial change.

The following is an example MCNP input deck for Section 3.5.

```
Model of 30% B HDPE 10-cm rad C
c
c target in air
c 6” cube (next time cubesat)
c DD 55eutron source
c Edited by Ryan Brockington
c
c +-------------------------------------------------+
c |                                                 |
c |                  Cell Cards                     |
c |                                                 |
c +-------------------------------------------------+
c # mat   density   surface        data
c
 3  1   -7.7       -3  imp:n,e,p 1 u=1   $Melamin block
52  16   -1.47     -52 3   imp:n,e,p 1 u=1  $ground base
 7  3    -2.3       -7    imp:n,e,p 1 u=1      $ vault
 8  6   -0.918      -8 18  imp:n,e,p 1 u=1     $ vault
18  3   -2.3        -18 9  imp:n,e,p 1 u=1     $ vault
 9  2   -0.00129  -9    imp:n,e,p 1 u=1        $air cavity
11  5   -5.06     -11    imp:n,e,p 1 u=1    $CeBr0
c 12  4   -11.3     -12    imp:n,e,p 1 u=1      $ extra Pb for CeBr
c air encasing
 31  2    -0.00129   -31  3 52 7 8 9 11   imp:n,e,p 1  u=1
 32  0     31                    imp:n,e,p 1  u=1
c room
 34  2    -0.00129   -32   imp:n,e,p 1 fill=1
 35  0               32   imp:n,e,p 0        $outside world
```

```
c +--------------------------------------------------+
c |                                                  |
c |                  Surface Cards                   |
c |                                                  |
c +--------------------------------------------------+
c # type params
c
 3   rpp  -5 5   -5 5     -5   0      $Melamin/TNT/DUT
 52  rpp  -50 50  -60 60  -80   0    $air/ground base
 7   rcc  0 0 30   0 0 10  30       $vault top   25cm shield
 8   rcc  0 0 10   0 0 20  30       $vault box   25cm shield
 18   rcc  0 0 10   0 0 20  10      $vault carbon   25cm shield
 9   rcc   0 0 10   0 0 20  2.5      $air/space inside vault
 11  rcc   30 0 10   10 0 0  3.81  $CeBr
c air background
31   rpp  -66 66      -86 76      -81 66
c room dimensions
32   rpp  -66.2 66.2  -86.2 76.2  -81.2 66.2


c +--------------------------------------------------+
c |                                                  |
c |                  Material Cards                  |
c |                                                  |
c +--------------------------------------------------+
c m# isotope    percent           $comment
 m2   6000       0.000150      $air 0.00129 g/cc
      7014       0.784431
      8016       0.210748
      18000      0.004671
```

```
m4   82000      1.0          $lead 11.34 g/cc
m1   28000      0.8          $NiCr 7.7 g/cc
     24000      0.2
m3   6012       1.0          $C   2.3 g/cc
m6   5010.70c   0.33         $BPE  bc2h4  0.918 g/cc
     6012       0.22
     1001.24    0.44
m5   58140.70c  0.25         $CeBr3  5.06 g/cc
     35079.70c  0.75
m16  8016       0.670604     $soil, U.S. Avg  1.47  O Si Al Fe Ca Na
     11023      0.005578
     12000      0.011432
     13027      0.053073
     14000      0.201665
     19000      0.007653
     20000      0.026664
     22000      0.002009
     25055      0.000272
     26000      0.021050
c
c +-----------------------------------------------------+
c |                                                     |
c |                  Source Definition                  |
c |                                                     |
c +-----------------------------------------------------+
sdef par=n  pos=0 0 11 erg=2.5
si1 0 1
sp1 -21
c
c +-----------------------------------------------------+
```

```
c |                                                  |
c |                  Data Cards                      |
c |                                                  |
c +--------------------------------------------------+
mode n p e
  PHYS:E 100 0 0 0 0 1 1 1 1 0
  PHYS:N
  PHYS:P
  cut:n j j 0 0
  cut:p j j 0 0 4
ptrac nps=1,1000 type=n file=asc event=bnk,sur,col,ter,cap
nps 68000000     $ 1M-1.8min originally 5000000
c
c +--------------------------------------------------+
c |                                                  |
c |                   Tallies                        |
c |                                                  |
c +--------------------------------------------------+
c
fc14 neutron flux
  f14:n  11 3
  e14 .00001 398log 3
fc24 neutron flux
  f24:n  11 3
  e24 0 398i 3
fc34 neutron flux
  f34:n  52
  e34 .000001 398log .01
fc44 photon flux
  f44:p  11 3
```

```
 e44 0 398i 11
fc16 neutron Edep averaged over the cell in MeV/g
 f16:n  11 3
 e16 0 398i 3
fc26 photon Edep averaged over the cell in MeV/g
 f26:p  11  3
 e26 0 398i 11
c
c +-------------------------------------------------+
c |                                                 |
c |                   Mesh                          |
c |                                                 |
c +-------------------------------------------------+
c
tmesh
c
c (a)radial meshes (b)zaxis(symmetry) (c)angles counterclockwise
c
c  flux=#/cm2     $dose=rem/hr    $pedep=MeV/cm3
c
c flux: flux
c pedep: total energy deposition/unit vol
c dose: dose over cross planes
c
rmesh1:n  flux pedep
c first layer area
cora1    -60  98i  60
corb1    -70  138i 70
corc1    -90       60
c
```

```
rmesh31:n  flux pedep
c first layer area
cora31    -60        60
corb31    -70   98i  70
corc31    -90  138i  60
c
rmesh21:n  flux pedep
c first layer area
cora21    -60  138i  60
corb21    -70        70
corc21    -90   98i  60
c
rmesh41:p  flux pedep
c first layer area
cora41    -60  138i  60
corb41    -70        70
corc41    -90   98i  60
c
endmd
```

Appendix F. MCNP Run Log

This appendix appears in its original form, without editorial change.

Breakdown of all the MCNP simulation runs conducted.

DATE	NAME	HISTORIES	TIME (min)		COMMENT
20220601	DUT1B30C10r2RB	50k	1.02		time for 50k histories
	DUT6B30C10r2RB	50k	0.99		check output files and data
					...3 Mh will take 1 hr
20220610	DUT1B30C10r2RB	3M	62.1		time for 3Mh. Update mesh
	DUT2B30C10r2RB	3M	61.51		Adjusted boundary, 12 layer
	DUT3B30C10r2RB	3M	61.85		
	DUT4B30C10r2RB	3M	60.77		
	DUT5B30C10r2RB	3M	60.65		Change Target layer in soil
	DUT6B30C10r2RB	3M	60.48		
	DUT7B30C10r2RB	3M	60.43		
	DUT8B30C10r2RB	3M	60.49		
	DUT9B30C10r2RB	3M	60.43		
	DUT10B30C10r2RB	3M	60.41		
	DUT11B30C10r2RB	3M	60.33		
	DUT12B30C10r2RB	3M	60.34		
220616	DUT5CebrSH10	200k	52.27	Curie	Calculate Photon Flux in CeBr
	DUT10CebrSH10	200k	52.2	Curie	... Insuffcient Histories
	DUT15CebrSH10	200k	83.84	Egale	six gamma sources
	DUT20CebrSH10	200k	82.69	Egale	
220617	DUT5CebrSH10	500k	207.21	Egale	More Histories
	DUT10CebrSH10	500k	207.1	Egale	five gamma sources
	DUT15CebrSH10	500k	206.52	Egale	
	DUT20CebrSH10	500k	207.31	Egale	
	DUT5Cebr_RSH10	3M	781.36	Curie	

220617	DUT5CebrSH0	8M		Egale	Move HDPE Shield down to soil
	DUT10CebrSH0	8M		Egale	...Bust Because forgot to change the
	DUT15CebrSH0	8M		Egale	six gamma sources
	DUT20CebrSH0	8M		Egale	
220617	DUT10CeBr20MhSH10	20M	5183.03	Curie	five gamma sources
					HDPE 10cm above soil
220622	DUT5CeBrh1M8SH0	1.8Mh	484.28	Curie	Re-run of 220617
	DUT10CeBrh1M8SH0	1.8Mh	487.53	Curie	Move HDPE Shield down to soil
	DUT15CeBrh1M8SH0	1.8Mh	774.15	Egale	...less photon flux detected in CeBr when the shielding is down

					Results: Shield height 10 cm and Detector height 10 cm
220623	DUT1SH10Ce10N11	9Mh	205.5	Egale	Moving the neutron source in different height
	DUT1SH10Ce10N15	9Mh	200.42	Egale	Sheild is at 10cm. Detector is at 10cm where it seems to
	DUT1SH10Ce10N19	9Mh	190.55	Egale	detect flux the best from the gamma runs
					... Position of the isotropic neutron source does not effect photon flux

220627	DUT1SH10Ce10N11_68Mh	68Mh	1535.11	25.58516667 Curie	More Histories, Serchiching for better photon flux
	DUT1SH10Ce10N15_68Mh	68Mh	2035.11	33.9185 Eagle	Neutron source, Sheild is at 10cm and CeBr is at 10cm
	DUT1SH10Ce10N19_68Mh	68Mh	2237.07	37.2845 Eagle	neutron source at 11cm, 15cm and 19cm to get the full spectrum of nflux to pflux ratio
					We hope to find which height for the neutron source ideal for optimal pflux and nflux

220701	DUT1SH10Ce10N11_68Mh_AIR	68Mh	556.24	curie	Instead of Soil we are using air
	DUT1SH10Ce10N15_68Mh_AIR	68Mh	706.71	curie	Neutron source, Sheild is at 10cm and CeBr is at 10cm
	DUT1SH10Ce10N19_68Mh_AIR	68Mh	826.51	curie	neutron source at 11cm, 15cm, and 19cm to get the full spectrum of nflux to pflux
					We want to compare how much neutron is being reflected from the soil reflection

220701	DUT1SH10Ce10N19_140Mh	50Mh (daily)	laptop	Goal is to figure out how many histories does it take to get the best photon flux
				incrementing by 50Mh for the wole week
				Using Soil
				Neutron source, Sheild is at 10cm and CeBr is at 10cm
				We want to get a better tally result from running more histores
220718	DUT1SH10CeBr10_Gamma	50Nh (daily)	Curie	Goal is to get a good gamma spectrum

Appendix G. Section Input File

This appendix appears in its original form, without editorial change.

Section 1: Shield Radius	Section 2: Target Depth	Section 3: CeBr3 Position
Air	DUT1B30C10r2RB	DUT5CeBr
DUT130B10gr3	DUT2B30C10r2RB	DUT10CeBr
DUT130B15gr3	DUT3B30C10r2RB	DUT15CeBr
DUT130B20gr3	DUT4B30C10r2RB	DUT20CeBr
DUT130B25gr3	DUT5B30C10r2RB	**Section 4: CeBr3 Position with Shield**
DUT130B30gr3	DUT6B30C10r2RB	DUT5CeBrh1M8SH0
DUT130B35gr3	DUT7B30C10r2RB	DUT10CeBrh1M8SH0
Soil	DUT8B30C10r2RB	DUT15CeBrh1M8SH0
DUT130B10r3	DUT9B30C10r2RB	**Section 5: Neutron Source Height**
DUT130B15r3	DUT10B30C10r2RB	**Soil**
DUT130B20r3	DUT11B30C10r2RB	DUT1SH10Ce10N11_68Mh
DUT130B25r3	DUT12B30C10r2RB	DUT1SH10Ce10N15_68Mh
DUT130B30r3	**Section 6: Discussion Gamma Sources**	DUT1SH10Ce10N19_68Mh
DUT130B35r3	**Air**	**Air**
	DUT1Sh10H2O10_Gamma_Air	DUT1SH10Ce10N11_68Mh_AIR
	Soil	DUT1SH10Ce10N15_68Mh_AIR
	DUT1Sh10CeBr10_Gamma	DUT1SH10Ce10N19_68Mh_AIR

Section 1: Shield Radius

Air

DUT130B10gr2

DUT130B15gr3

DUT130B20gr4

DUT130B25gr5

DUT130B30gr6

DUT130B35gr7

Soil

DUT130B10r2

DUT130B15r3

DUT130B20r4

DUT130B25r5

DUT130B30r6

DUT130B35r7

Section 2: Target Depth

DUT1B30C10r2RB

DUT2B30C10r2RB

DUT3B30C10r2RB

DUT4B30C10r2RB

DUT5B30C10r2RB

DUT6B30C10r2RB

DUT7B30C10r2RB

DUT8B30C10r2RB

DUT9B30C10r2RB

DUT10B30C10r2RB

DUT11B30C10r2RB

DUT12B30C10r2RB

Section 3: $CeBr_3$ Position

DUT5CeBr

DUT10CeBr

DUT15CeBr

DUT20CeBr

Section 4: $CeBr_3$ Position with Shield

DUT5CeBrh1M8SH0

DUT10CeBrh1M8SH0

DUT15CeBrh1M8SH0

Section 5: Neutron Source Height

Soil

DUT1SH10Ce10N11_68Mh

DUT1SH10Ce10N15_68Mh

DUT1SH10Ce10N19_68Mh

Air

DUT1SH10Ce10N11_68Mh_AIR

DUT1SH10Ce10N15_68Mh_AIR

DUT1SH10Ce10N19_68Mh_AIR

Section 6: Discussion Gamma Sources

Neutron Source

DUT1SH10Ce10N19_140Mh (GC11)

Gamma Air

DUT1Sh10H2O10_Gamma_Air

Gamma Soil

DUT1Sh10CeBr10_Gamma

List of Symbols, Abbreviations, and Acronyms

B	boron
$CeBr_3$	cerium(III) bromide
DD	deuterium–deuterium
FOM	figure of merit
GRS	gamma ray spectrometer
H	hydrogen
HDPE	high-density polyethylene
LEND	Lunar Exploration Neutron Detector
LRO	Lunar Reconnaissance Orbiter
MCNP	Monte Carlo N-Particle Transport
NASA	National Aeronautics and Space Administration
nFlux	neutron flux
NS	neutron spectrometer
PDF	probability distribution function
pFlux	photon flux
TVL	tenth-value layer

1 (PDF) DEFENSE TECHNICAL INFORMATION CTR DTIC OCA

1 (PDF) DEVCOM ARL FCDD RLB CI TECH LIB

1 (PDF) DEVCOM ARL FCDD RLA GC M LITZ